الجمهورية الجزائرية الديمقراطية الشعبية
People's Democratic Republic of Algeria
وزارة التعليم العالي والبحث العلمي
Ministry of Higher Education and Scientific Research

BADJI MOKHTAR -ANNABA UNIVERSITY
UNIVERSITE BADJI MOKHTAR ANNABA

جامعة باجي مختار - عنابة -

Sciences Faculty

Year : 2021/2022

Departement of Mathematics

THESIS

Submitted for the obtention of diploma of
Doctorat in Sciences

Numericals methods in domains of geometrics dimensions

In Field
Applied Mathematics
By
Salim Adjemi

First Supervisor: Ahmed Berkane Pr. U.B.M. ANNABA

Second Supervisor: Salah Zitouni M.C.A. U. SOUK-AHRAS

Examination Committee Members:

Chairman:	Abdelhak DJEBABLA	Pr.	U.B.M. ANNABA
Examinator:	Elbahi HADIDI	Pr.	U.B.M. ANNABA
Examinator:	Lamine BOUZETTOUTA	M.C.A.	U. SKIKDA
Examinator:	Houssem Eddine KHOCHEMANE	M.C.A	E.N.S.E.T. SKIKDA

Dedication

To my dear wife, who supported me through thick and thin and was my best support in all adversities and stumbles, I dedicate this work to you as a token of love and affection.

Thanks

I would like to thank Pr. A. Djebabla for his interest in this work and for the honor he does me to chair the jury. I would also like to thank Messrs. Pr. E. Hadidi, Dr. H. E. Khochemane and Dr. L. Bouzettouta for their attention to this thesis and for their participation on the jury.

I would particularly like to thank my supervisor, pr. A. Berkane and Dr. S. Zitouni, for suggesting this subject to me and for guiding me in my training in Mathematics.

Finally, I dedicate this work to my family and all my friends from near and far.

مـــــلخص

تهدف هذه الأطروحة إلى دراسة نظام بريس- تيموشينكو اللاخطي ذي البعد الواحد مع الصوت الثاني، حيث يكون التوصيل الحراري المصاغ بقانون كاتانيو في المعادلة الثانية.ولقد أثبتنا أن هذا النظام مستقر بشكل كبير باستخدام طريقة الطاقة التي تتطلب بناء دالة ليابونوف مناسبة بواسطة استغلال طريقة المضاعفات.

علاوة على ذلك،فإن النتيجة لا تعتمد على أي شرط على معاملات النظام وتحققنا من صحة نتائجنا النظرية من خلال إجراء بعض التقديرات العددية باستخدام مخطط أويلر الضمني بالنسبة إلى الزمن وطريقة العناصر المنتهية بالنسبة للفضاء.

الكلمات المفتاحية:

نظام بريس- تيموشنكو اللاخطي ، الصوت الثاني ، التناقص الأسي ، طريقة الطاقة ، التقريب العددي ، طريقة العناصر المنتهية .

Abstract

This thesis aims to study the one dimensional nonlinear Bresse-Timoshenko system with second sound where the heat conduction given by Cattaneo's law is effective in the second equation. We prove that the system is exponentially stable by using the energy method that requires constructing a suitable Lyapunov functional through exploiting the multipliers method. Furthermore, the result does not depend of any condition on the coefficients of the system. Finally, we validate our theoretical result by performing numerical approximations based on the standard finite element method, using the retrograde Euler scheme for temporal and spatial discretization.

Keywords: Nonlinear Bresse-Timoshenko system, second sound, exponential decay , energy method, numerical approximation, finite elements method.

Résumé

Cette thése a pour but d'étudier le systéme de Bresse-Timoshenko non linéaire unidimensionnel avec second son oé la conduction thermique donnée par la loi de Cattaneo est effective dans la seconde équation. Nous prouvons que le systéme est exponentiellement stable en utilisant la méthode de l'énergie qui nécessite la construction d'une fonctionnelle de Lyapunov appropriée en exploitant la méthode des multiplicateurs. De plus, le résultat ne dépend d'aucune condition des coefficients du systéme. Enfin, nous validons notre résultat théorique en effectuant des approximations numériques basées sur la méthode standard des éléments finis, en utilisant le schéma d'Euler rétrograde pour la discrétisation temporelle et spatiale.

Mots clés: Systéme non linéaire de Bresse-Timoshenko, second son, décroissance exponentielle, méthode de l'énergie, approximation numérique, méthode des éléments finis.

Contents

Notations

In what follows, we will use the following notations:

$\mathbb{R}^N$ N-dimensional real Euclidean space.

Ω bounded open of $\mathbb{R}^N$.

$\partial\Omega$ border of Ω.

p_i a real number greater than or equal to 1 for all $i = 1, \ldots, N$.

$p_- = \min\{p_i, \quad i = 1, 2, \ldots, N\}$.

$p_+ = \max\{p_i, \quad i = 1, 2, \ldots, N\}$.

p_i' conjugate of p_i, that is to say $\dfrac{1}{p_i} + \dfrac{1}{p_i'} = 1$.

$\hookrightarrow\hookrightarrow$ injection compact.

$\overline{p}$ the harmonic mean of p_i, that is to say $\dfrac{1}{\overline{p}} = \dfrac{1}{N}\sum_{i=1}^{N}\dfrac{1}{P_i}$.

$\overline{q}^* = \dfrac{N\overline{q}}{N - \overline{q}}$.

a.e. almost everywhere.

$|E|$ measure of the set E, when its Lebesgue measure is finite.

$\mathrm{supp}(f)$ function support f.

K_{Comp} K compact.

$\mathcal{M}(\Omega)$ set of Radon measurements bounded on Ω.

$D_i u = \frac{\partial u}{\partial x_i}$.

$Du = (D_1 u, D_2 u, \ldots, D_N u)$.

$\nabla u = \left(\frac{\partial u}{\partial x_1}, \frac{\partial u}{\partial x_2} \ldots \frac{\partial u}{\partial x_N}\right) = \mathrm{grad}\ \ u$.

$\mathrm{div}(v) = \sum_{i=1}^{N} D_i v_i$, $v = (v_1, \ldots, v_N)$.

χ_E characteristic function of the set E.

$$S_\nu(\sigma) = \begin{cases} \mathrm{sign}(\sigma), & \text{if} \quad |\sigma| > \nu \\ \dfrac{\sigma}{\nu}, & \text{if} \quad |\sigma| \leq \nu. \end{cases}$$

$$\forall \sigma \in \mathbb{R}, \text{sign}(\sigma) = \begin{cases} 1, & \text{if} \quad \sigma > 0 \\ 0, & \text{if} \quad \sigma = 0 \\ -1, & \text{if} \quad \sigma < 0. \end{cases}$$

T_k the truncation at height k defined by $T_k(t) = \begin{cases} t, & \text{if} \quad |t| \leq k \\ \dfrac{kt}{|t|}, & \text{if} \quad |t| > k. \end{cases}$

Y' topological dual of the topological vector space Y.

$\mathcal{D}(\Omega)$ the space of test functions (the space of functions $C^\infty(\Omega)$ with compact support included in an open Ω of $\mathbb{R}^N$).

$L^p(\Omega) = \left\{ u : \Omega \longrightarrow \mathbb{R} \quad \text{mesurable}; \int_\Omega |u|^p < \infty \right\}$ endowed with the norm $\| u \|_p = \left(\int_\Omega |u|^p \right)^{\frac{1}{p}}$.

$L^\infty(\Omega) = \left\{ u : \Omega \longrightarrow \mathbb{R}, \text{measurable}; \ \sup_\Omega \text{ess} |u| < \infty \right\}$ provided with the standard $\| u \|_\infty = \sup_\Omega \text{ess} |u|$.

$W^{1,p}(\Omega) = \left\{ u \in L^p(\Omega); \ \nabla u \in L^p(\Omega) \right\}$ provided with the standard $\|u\|_{W^{1,p}(\Omega)} = \|u\|_{L^p(\Omega)} + \|\nabla u\|_{L^p(\Omega)}$.

$W_0^{1,p}(\Omega) = \left\{ u \in L^p(\Omega); \nabla u \in (L^p(\Omega))^N \quad \text{and} \ \ u = 0 \text{ on } \partial\Omega \ \right\}$.

$L^{\vec{p}}(\Omega) = L^{p_1}(\Omega) \times L^{p_2}(\Omega) \times \ldots \times L^{p_N}(\Omega) = \prod_{i=1}^N L^{p_i}(\Omega)$, with $p_i > 1$.

$\|v\|_{X^{1,\vec{p}}(\Omega)} = \sum_{i=1}^N (\|v\|_{L^{p_i}} + \|D_i v\|_{L^{p_i}})$.

$\overline{\mathcal{D}(\Omega)} = X_0^{1,\vec{p}}(\Omega) = \left\{ v \in X^{1,\vec{p}}(\Omega) \quad \text{such as} \quad v = 0 \ \text{ on } \ \partial\Omega \right\} \subseteq W_0^{1,\vec{p}}(\Omega)$.

$W_{x_i,0}^{1,p_i}(\Omega) = \overline{\mathcal{D}(\Omega)}^{\|\cdot\|_i}$ with $\|u\|_i = \|u\|_{L^{p_i}(\Omega)} + \|D_i u\|_{L^{p_i}(\Omega)}$.

$W_0^{1,\vec{p}}(\Omega) = \left\{ u \in L^{p_i}(\Omega) \quad \text{and} \quad \frac{\partial u}{\partial x_i} \in L^{p_i}(\Omega) \quad \text{with} \quad u = 0 \quad \text{on} \quad \partial\Omega \quad \forall i = 1, \ldots, N \right\}$.

Introduction

In the present thesis, we will interpret the numerical results that obtain using the finite element method and establish an error estimate the finite element method has become one of the most important useful engineering tools for engineers and scientists. This work presents introductory andsome advanced topics of the Finite Element Method (FEM). Finite element theories,formulations and various example programs written in MATLAB are presented. The work is written as a text work for upper level undergraduate and lower level graduatecourses, as well as a reference work for engineers and scientists who want to writequick finite element analysis programs.

We consider the following one dimensional nonlinear Bresse-Timoshenko system with second sound

$$\begin{cases} \rho_1\varphi_{tt} - k\left(\varphi_x + \psi\right)_x + \mu_1\varphi_t = 0 & \text{in} \quad (0,1)\times(0,\infty), \\ -\rho_2\varphi_{ttx} - b\psi_{xx} + k\left(\varphi_x + \psi\right) + \gamma\theta_x + \mathrm{f}\left(\psi\right) = 0 & \text{in} \quad (0,1)\times(0,\infty), \\ \rho_3\theta_t + kq_x + \gamma\psi_{tx} + \lambda\theta = 0 & \text{in} \quad (0,1)\times(0,\infty), \\ \tau_0 q_t + \delta q + k\theta_x = 0 & \text{in} \quad (0,1)\times(0,\infty). \end{cases} \tag{1}$$

With the initial and boundary conditions

$$\begin{cases} \varphi(x,0) = \varphi_0(x), \varphi_t(x,0) = \varphi_1(x), \psi(x,0) = \psi_0(x) & \text{in} \quad (0,1), \\ \psi_t(x,0) = \psi_1(x), \theta(x,0) = \theta_0(x), q(x,0) = q_0(x) & \text{in} \quad (0,1), \\ \varphi(0,t) = \varphi(1,t) = \psi(0,t) = \psi(1,t) = q(0,t) & \\ = q(1,t) = \theta(0,t) = \theta\left(1,t\right) = 0 & \text{in} \quad (0,\infty), \end{cases} \tag{2}$$

where $t \in (0,+\infty)$ denotes the time variable and $x \in (0,1)$ is the space variable along with the beam of length L, in its equilibrium configuration. Here φ, ψ, θ, q and f(ψ) are specific functions represent, respectively, the transverse displacement of the beam, the rotation angle, the

different temperature, the heat flux and forcing term. The coefficients ρ_1, ρ_2, ρ_3, μ_1, τ_0, δ, γ, b, k and λ are positive constants represent the constitutive parameters defining the coupling among the defferent conponents of the materials.

From physical point of view, it is well known that the model using the classic Fourier's law leads to the physical paradox of infinite speed of heat propagation. Many theories have subsequently emerged, to overcome this physical paradox but still keeping the essentials of a heat conduction process. One of which is the advent of the second sound effects observed experimentally in materials at a very low temperature. Second sound effects arise when heat is transported by a wave propagation process instead of the usual diffusion. This theory suggests replacing the classic Fourier's law $\gamma\theta_x + q$, where γ is the coefficient of thermal conductivity and q is the heat flux by a modified law of heat conduction called Cattaneo's law $\gamma\theta_x + q + \tau q_t$. Here, the parameter $\tau > 0$ represents the relaxation time describing the time lag in the response of the heat flux to a gradient in the temperature. The obtained heat system is of hyperbolic type and hence, automatically, eliminating the paradox of infinite speeds. Among the works that have been realised in this fiéeld, we refer the reader to [34, 35]. In the following Figure we introduce the displacements and the rotation angle in the (x_1, x_3) plane as well as the temperature distribution with its contribution to the deformation of the beam as showing in many works for instance [10] where

- $u = u(x_1, t)$: the longitudinal displacement of points lying on the x_1-axis,
- $\psi = \psi(x_1, t)$: the angle of rotation for the normal to the x_1-axis,

Θ is the Taylor's expansion for the temperature distribution in the (x_1, x_3)-plane (with $x_2 = 0$):

$$\Theta(x_1, x_3, t) = \Theta(x_1, 0, x_3, t) = \theta_1(x, t) + x_3\theta_3(x, t)$$

where θ_1 and θ_3 are temperature components (functions) that may represent the temperature deviations from the reference temperature Θ_0 along the longitudinal and vertical directions.

Elishakoff et al. [27, 28], gave a brief description on the beam model in one-dimensional for beam vibrations. The classical Bernoulli-Euler differential equation ignores rotational inertia and shear deformation. It is given by

$$EI\varphi_{xxxx} + \rho A\varphi_{tt} = 0, \tag{3}$$

where E is the modulus of elasticity, I is the moment of inertia, $\varphi(x, t)$ is the transverse

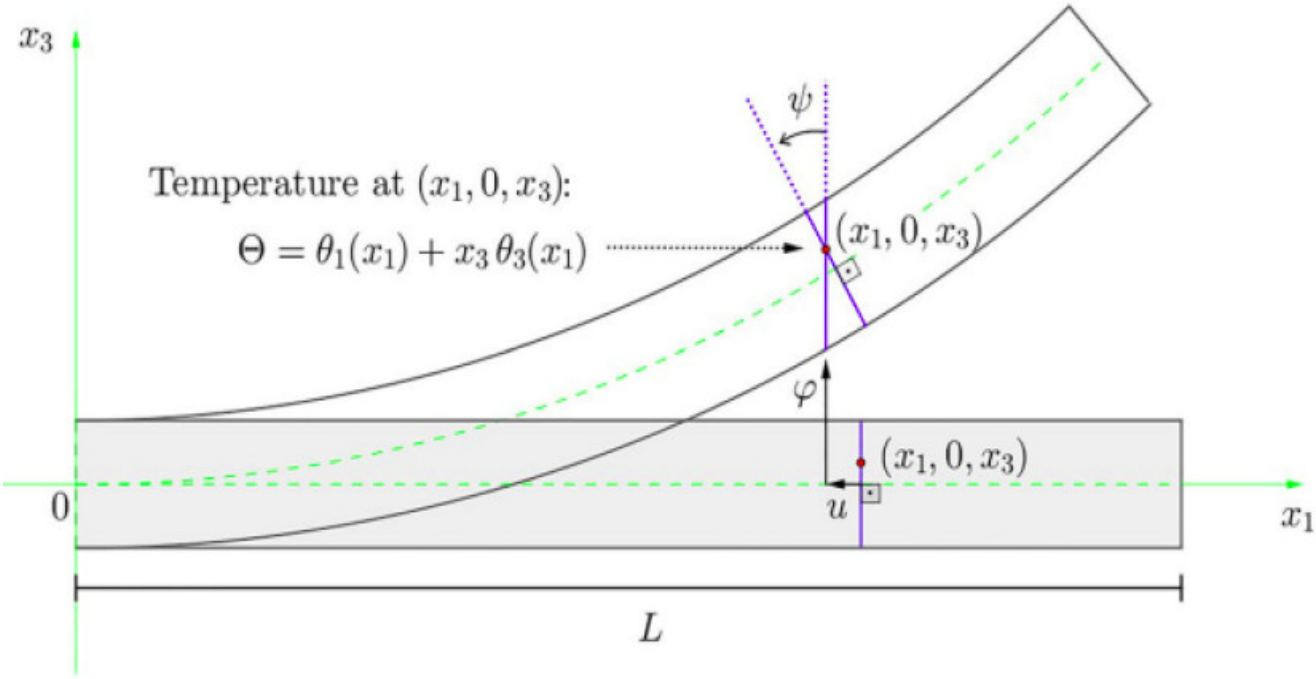

Displacements, rotation angle and temperature distribution in the (x_1, x_3)-plane

displacement, x is the axial coordinate, t is the time, ρ is the material density, and A is the cross-sectional area.

Later, Bresse [19] and Rayleigh extended and corrected the Bernoulli-Euler equation (3), by taking into account the rotary movement of the beam elements. The angle of rotation equals the slope of the deflection curve φ_x, the associated angular acceleration is φ_{xtt}. As a result, the moment of inertia of the element about an axis through its center of mass equals $\rho I \varphi_{xtt} dx$ and according to D'Alembert's principle, we obtain

$$-V + M_x - \rho I \varphi_{xtt} = 0, \tag{4}$$

where $V(x,t)$ is the shearing force and $M(x,t)$ the bending moment.

Replacing this equation in the case of dynamic equilibrium with the forces of transverse vibration, we have

$$V_x = -\rho A \varphi_{tt} = (M_x - \rho I \varphi_{xtt})_x. \tag{5}$$

Physically from elastic theory, we have $M = EI\varphi_{xx}$, then it results in a Rayleigh model for the uniform beam oscillations given by

$$EI\varphi_{xxxx} + \rho A\varphi_{tt} - \rho I\varphi_{xxtt} = 0, \tag{6}$$

we call equation (6) the rotatory inertial.

Afterwards, Timoshenko [48] extended the equation (6) by adding the impact of the shear deformation, expressing the slope of the deflection curve in two parts

$$\varphi_x = -\psi + \zeta, \tag{7}$$

ψ as the rotation of the cross-sections with the neglection of the shear deformation and ζ as the angle associated with the shear deformation at the neutral axis in the same cross-section. On the other hand, according to the mechanics of solid we can write

$$M = EI\psi_x, \tag{8}$$

$$V = k_1\zeta AG = k_1 AG(\varphi_x + \psi), \tag{9}$$

where k_1 is the shear coefficient and G is the shear modulus.

The state of dynamic equilibrium of forces in the vertical direction is given by

$$\rho A\varphi_{tt} - V_x = 0. \tag{10}$$

Deriving with respect to the in equation (7) and by substituting in the dynamic equilibrium equation of motion (4), we get

$$-V + M_x + \rho I\psi_{tt} = 0. \tag{11}$$

The Timoshenko system, was obtained by substituting respectively (9) and (8) into (10) and (11), thus

$$-k_1 AG(\varphi_x + \psi)_x + \rho A\varphi_{tt} = 0. \tag{12}$$

$$-k_1 AG(\varphi_x + \psi) + EI\psi_{xx} + \rho I\psi_{tt} = 0, \tag{13}$$

where,

$\rho_1 = \rho A$ is the mass density,

$\rho_2 = \rho I$ is the moment mass inertia,

$b = EI$ is the rigidity coefficient (of the cross-section),

$k = k_1 AG$ is the shear modulus of elasticity.

Then, the Timoshenko system takes the following form

$$\begin{cases} \rho_1 \varphi_{tt} - k\left(\varphi_x + \psi\right)_x = 0, \\ \rho_2 \psi_{tt} - b\psi_{xx} + k\left(\varphi_x + \psi\right) = 0. \end{cases} \tag{14}$$

It should be noticed that mentioned problem plays a crucial role in engineering applications. And for more details on the valuable resources that have been realised regarding Timoshenko system, we refer the readers to [5, 11, 12, 13, 14, 15, 16, 30, 33, 38, 39, 48, 52].

Elishakoff [26], by differentiating the Timoshenko hypotheses (7) with respect to t, we get

$$\psi_{tt} = -\varphi_{ttx}. \tag{15}$$

Inserting (15) in $(14)_2$, we obtain the well-known Bresse-Timoshenko system by combining d'Alembert's concept for dynamic equilibrium, with Timoshenko hypothesis to get the following system

$$\begin{cases} \rho_1 \varphi_{tt} - k\left(\varphi_x + \psi\right)_x = 0, \\ -\rho_2 \varphi_{ttx} - b\psi_{xx} + k\left(\varphi_x + \psi\right) = 0. \end{cases} \tag{16}$$

For more details, we refer [8, 9, 22, 26, 29].

Many investigations have been realised concerning the asymptotic behavior of the solution of Bresse-Timoshenko system. Among them, we cite the work of Almeida and Ramos [6], who they considered the following system

$$\begin{cases} \rho_1 \varphi_{tt} - \beta\left(\varphi_x + \psi\right)_x = 0, \\ -\rho_2 \varphi_{ttx} - b\psi_{xx} + \beta\left(\varphi_x + \psi\right) + \mu_1 \psi_t = 0, \end{cases} \tag{17}$$

where they showed that the viscous damping acting on angle rotation of the above system is strong enough to provoke an exponential decay of the solution. Junior et al. [7] considered the following system

$$\begin{cases} \rho_1 \varphi_{tt} - \beta\left(\varphi_x + \psi\right)_x + \mu_1 \psi_t = 0, \\ -\rho_2 \varphi_{ttx} - b\psi_{xx} + \beta\left(\varphi_x + \psi\right) = 0, \end{cases} \tag{18}$$

and they showed that the mechanism damping given by the viscous damping acting on the transverse displacement of the beam stabilizes exponantially the system.

Kh. Zennir et al. [51] studied the following nonlinear Bresse-Timoshenko system

$$\begin{cases} \rho_1 \partial_{tt}\varphi - k\left(\varphi_x + \psi\right)_x + \sigma_1 \partial_t \varphi = 0, \\ -\rho_2 \partial_{tt}\varphi_x - \alpha \psi_{xx} + k\left(\varphi_x + \psi\right) - \xi_1 \theta_x \\ \qquad -\xi_2 p_x + \sigma_2 \mathcal{G}(\partial_t \psi) = 0, \\ c\partial_t \theta + d\partial_t p - k\theta_{xx} - \xi_1 \partial_t \psi_x = 0, \\ d\partial_t \theta + r\partial_t p - h p_{xx} - \xi_2 \partial_t \psi_x = 0. \end{cases} \tag{19}$$

The authors proved the well-posedness of the system by using the classical Faedo-Galerkin approximations and showed a general decay result of the system.

Motivated by the previous works, in this thesis we give a global existence and regularity results, which can be proved by using the standard Feado-Galerkin method. Moreover, we show that the dissipation given by the second sound is strong enough to give an exponential stability of solution of the system (1) by using the energy method, that requires to constract an appropriate Lyapunov functional which allows us to estimate the energy of the system (1) and to show that it decays an exponetial manner without any conditions on the coefficients of the system. Importance of this complimantary control and his influence on the asymptotic behavior of the solution appears in many works for the different types of problems such as [11, 31, 33]. Finally, we will interpret the numerical results that we will obtain using the finite element method and we will establish an error estimate.

Chapter 1

Basic notions and numerical method

In this chapter we shall introduce and state some necessary materials needed in the proof of our results, and shortly the basic results which concerning the Banach spaces, the weak and weak star topologies, the L^p space, Sobolev spaces and other theorems. The knowledge of all this notations and results are important for our study.

1.1 Functional spaces

The spaces L^p and Sobolev spaces are a ubiquitous tool in the study of elliptic and parabolic partial differential equations.

Understanding them is therefore a necessary step before tackling the equations in question.

We take up in this section certain statements of H. Brezis [21] on the subject. For a more complete presentation of Sobolev spaces, one can consult the work of R. A. Adams [1].

In what follows, we denote by Ω a regular bounded open set of $\mathbb{R}^N$ and $\mathcal{D}(\Omega)$ the space of class functions $\mathcal{C}^\infty$ with compact support in Ω. We note by $L^p(\Omega)$, the Lebesgue space with $1 \leq p < \infty$ defined by:

$$L^p(\Omega) = \left\{ u : \Omega \longrightarrow \mathbb{R} \quad \text{mesurable}; \int_\Omega |u|^p < \infty \right\}, \tag{1.1}$$

with the norm:

$$\| u \|_p = \left(\int_\Omega |u|^p \right)^{\frac{1}{p}}, \tag{1.2}$$

and for $p = \infty$, we notice:

$$L^{\infty}(\Omega) = \left\{ u : \Omega \longrightarrow \mathbb{R} \quad \text{mesurable}; \ \sup_{\Omega} \operatorname{ess} |u| < \infty \right\}, \tag{1.3}$$

that we is the norm:

$$\| u \|_{\infty} = \sup_{\Omega} \operatorname{ess} |u|. \tag{1.4}$$

Fundamental lemmas and theorems

Lemma 1.1.1 (Fatou's lemma). *H.Brézis [21]*

That is $(f_n)_n$ *a sequence of functions* $L^1(\Omega)$ *such as:*

(1) *for each* $n, f_n(x) \geq 0$ a.e. sur Ω

(2) $\sup_n \int_{\Omega} f_n < \infty,$

for each $x \in \Omega$ *we pose* $f(x) = \liminf_{n \to \infty} f_n(x)$.

So $f \in L^1(\Omega)$ *and*

$$\int_{\Omega} f \leq \liminf_{n \to \infty} \int_{\Omega} f_n.$$

Theorem 1.1.2 (Beppo Levi's monotone convergence theorem [21]).

That is $(f_n)_n$ *a growing suite of functions of* $L^1(\Omega)$ *such as* $\sup_n \int f_n < \infty$.

So $f_n(x)$ *converges* a.e. on Ω *to a finite limit noted* $f(x)$, *what's more*

$$f \in L^1(\Omega) \text{ and } ||f_n - f||_{L^1(\Omega)} \longrightarrow 0.$$

Theorem 1.1.3 (Minkowski inequality [21]).

Let (Ω, τ, μ) *a measured space and* p *a satisfying real number,* $1 \leq p < +\infty$, $f : \Omega \longrightarrow \mathbb{R}$ *such as* $f \in L^p(\Omega)$, *if* $f_1, f_2, \ldots, f_n \in L^p(\Omega, \mathbb{R})$ *then:*

$$\sum_{k=1}^{N} f_k \in L^p(\Omega, \mathbb{R}) \quad \text{et} \quad \left(\int_{\Omega} \left| \sum_{k=1}^{N} f_k(x) \right|^p d\mu(x) \right)^{\frac{1}{p}} \leq \sum_{k=1}^{N} \left(\int_{\Omega} |f_k(x)|^p \, d\mu(x) \right)^{\frac{1}{p}},$$

gold:

$$\left\| \sum_{k=1}^{N} f_k(x) \right\|_p \leq \sum_{k=1}^{N} \| f_k(x) \|_p .$$

Theorem 1.1.4 (Lebesgue dominated convergence theorem [21]).

That is (f_n) *a sequence of measurable functions which converges to* f a.e. dans Ω.

We assume that there is $g \in L^1(\Omega)$ *such as* $\forall n \geq 1,\ |f_n(x)| \leq g(x)$, a.e. $x \in \Omega$. *So* $f \in L^1(\Omega)$ *and*

$$\lim_{n\to+\infty} \int_\Omega |f_n - f| dx = 0, \lim_{n\to+\infty} \int_\Omega f_n dx = \int_\Omega f dx.$$

Theorem 1.1.5 (Partial reciprocal of the dominated convergence theorem[21]).

That is $1 \leq p < +\infty$, $f \in L^p(\Omega)$ et $(f_n) \subset L^p(\Omega)$ *such as* $\lim_{n\to+\infty} \| f_n - f \|_p = 0$ *il existe a function* $g \in L^p(\Omega)$ *and a sub-sequence* $(f_{n_k})_k$ *such as:*

$$|f_{n_k}| \leq g \text{ a.e. }, \quad \text{et } f_{n_k} \longrightarrow f \text{ a.e.}$$

Lemma 1.1.6. *[36]*

That is (Ω, τ, μ) *is a measured space and* (f_n)*it is a sequence of measurable functions of* Ω *in* $\mathbb{R}$ *we say that* (f_n) *is a Cauchy sequence in measure if and only if:*

$$\forall \varepsilon > 0, \forall \eta > 0, \exists n_0 \in \mathbb{N} \quad \text{such as} \quad p, q > n_0 \Rightarrow \text{mes}\Big\{ x \in \Omega : |f_p(x) - f_q(x)| > \varepsilon \Big\} \leq \eta. \quad (1.5)$$

1.2 Reminder on Sobolev spaces

In this part we will present some definitions and properties of Sobolev spaces,
see [1] and [43].

Sobolev's space $W^{1,p}(\Omega)$

Let $\Omega \subset \mathbb{R}^N$ be an open domain and $1 \leq p \leq \infty$. Space :

$$W^{1,p}(\Omega) = \Big\{ u \in L^p(\Omega);\ \nabla u \in L^p(\Omega) \Big\},$$

Also, we denote by

$$\|u\|_{W^{1,p}(\Omega)} = \|u\|_{L^p(\Omega)} + \|\nabla u\|_{L^p(\Omega)}, \quad (1.6)$$

is a Banach space, separable and reflexive for $1 < p < \infty$.

We denote by $\mathcal{C}_0^\infty(\Omega)$ all functions $\mathcal{C}^\infty$ with compact support in Ω is noted $\mathcal{D}(\Omega)$.

We can also define $W_0^{1,p}(\Omega)$ like the adhesion of $\mathcal{D}(\Omega)$ in $W^{1,p}(\Omega)$, by the following definition:

$$W_0^{1,p}(\Omega) = \Big\{ u \in L^p(\Omega); \nabla u \in (L^p(\Omega))^N, \quad \text{and} \quad u = 0 \text{ on } \partial\Omega \Big\}. \quad (1.7)$$

Proposition 1.2.1.

1. *Space* $W^{1,p}(\Omega)$ *is a Banach space, for all* $1 \leq p \leq +\infty$.

2. *Space* $W^{1,p}(\Omega)$ *is a reflective space, for all* $1 < p < +\infty$.

3. $W^{1,p}(\Omega)$ *separable if* $1 \leq p < +\infty$.

4. *Whether* $p = 2$, *then* $W^{1,2}(\Omega) = H^1(\Omega)$ *is a Hilbert space for the inner product.*

$$(u, v) \longmapsto (u|v) = \int_\Omega uvdx + \sum_{i=1}^{N} \int_\Omega \frac{\partial u}{\partial x_i}.\frac{\partial v}{\partial x_i}dx. \tag{1.8}$$

1.3 The Faedo-Galerkin method

The Faedo-Galerkin method consists of performing the following steps:

(i) Write the problem in variational form,

(ii) Looked for approximate solutions in finite dimensional spaces,

(iii) Establish a priori estimates on these approximate solutions,

(iv) Passing to the limit, thanks to compactness properties,

(v) Verification that this limit is a solution to the problem.

1.4 Injections and inequalities

Theorem 1.4.1 (Rellich-Kondrachov theorem [17]).

We assume Ω *of class* $\mathcal{C}^1$ *and* $p < N$ *then:*

$$W^{1,p}(\Omega) \hookrightarrow\hookrightarrow L^p(\Omega), \forall p \in [1, p^*[$$

Where $p^* = \frac{Np}{N-p}$. *Especially,* $W^{1,p}(\Omega) \hookrightarrow\hookrightarrow L^p(\Omega)$, *for everything* $p \in [1, +\infty)$.

Theorem 1.4.2 (Injection of Sobolev-case $p < N$ [21]).

That is $\Omega \subset \mathbb{R}^N$ *a bounded open set and* $1 \leq p \leq N$, *then*

$$W^{1,p}(\Omega) \text{ continuously injects itself into } L^{\frac{Np}{N-p}}(\Omega).$$

Inequalities of Sobolev, Hölder, Poincaré and Young (See [1, 21]).

Theorem 1.4.3 (Sobolev inequality).

be $\Omega = \mathbb{R}^N$ Where Ω is an open of $\mathbb{R}^N$ whose border is regular and $1 \leq p < N$,then $W^{1,p}(\Omega) \hookrightarrow L^{p^\star}(\Omega)$ où $\frac{1}{p^\star} = \frac{1}{p} - \frac{1}{N}$, with continuous injection. Furthermore

$$||u||_{L^{p^*}(\Omega)} \leq C||\nabla u||_{L^p(\Omega)}.$$

Theorem 1.4.4 (Hölder's inequality).

Let Ω an open of $\mathbb{R}^N$, $1 < p < \infty$, $f \in L^p(\Omega)$ and $g \in L^{p'}(\Omega)$ with $\frac{1}{p} + \frac{1}{p'} = 1$. So $f.g \in L^1(\Omega)$ and

$$\int_\Omega |fg|dx \leq ||f||_{L^p(\Omega)}||g||_{L^{p'}(\Omega)}.$$

Theorem 1.4.5 (Poincaré inequality).

We think that Ω is a bounded open set. Then there is a constant C (depends on Ω and if p) such as:

$$||u||_{L^p(\Omega)} \leq C||\nabla u||_{L^p(\Omega)}, \forall u \in W_0^{1,p}(\Omega), (1 \leq p < \infty).$$

In particular the expression $||\nabla u||_{L^p(\Omega)}$ is a standard on $W_0^{1,p}(\Omega)$,which is equivalent to the norm $||u||_{W^{1,p}(\Omega)}$, on $H_0^1(\Omega)$.
The phrase, $\int_\Omega \nabla u \nabla v$ is a scalar product which induces the norm $||\nabla u||_{L^2(\Omega)}$ equivalent to the standard $||u||_{H^1(\Omega)}$.

Remark 1.4.6. Poincaré's inequality holds if Ω is of finite measure or Ω is bounded in one direction.

Theorem 1.4.7 (Young's inequality).

$$\forall\, a \in \mathbb{R}, \forall\, b \in \mathbb{R} : |a.b| \leq \frac{|a|^p}{p} + \frac{|a|^q}{q}, \quad \left(\frac{1}{p} + \frac{1}{q} = 1, p > 1, q > 1\right).$$

We will also some times use:

$$\forall a \geq 0, \forall b \geq 0, \quad a.b = (p\varepsilon)^{\frac{1}{p}} a.(p\varepsilon)^{-\frac{1}{p}} b$$

$$a.b \leq \varepsilon a^p + \frac{\left((p\varepsilon)^{-\frac{1}{p}} b\right)^q}{q}$$

$$a.b \leq \varepsilon a^p + (p\varepsilon)^{-\frac{1}{p-1}} b^q \left(1 - \frac{1}{p}\right)$$

$$a.b \leq \varepsilon a^p + (p\varepsilon)^{-\frac{1}{p-1}} \left(1 - \frac{1}{p}\right) b^q.$$

Also in the form:

$$\forall a \geq 0, \forall b \geq 0, \quad a.b = (\frac{a}{\varepsilon})(\varepsilon b) \leq \frac{1}{p}(\frac{a}{\varepsilon})^p + \frac{1}{q}(\varepsilon b)^q,$$

with $\varepsilon > 0$.

Remark 1.4.8.

$$\left(\sum_{i=1}^{N} a_i\right)^k \leq max\{1, N^{k-1}\} \sum_{i=1}^{N} a_i^k.$$

So:

$$\left(\sum_{i=1}^{N} a_i^{p_+}\right)^{\frac{1}{p_+}} \leq max\{1, N^{\frac{1}{p_+}-1}\} \sum_{i=1}^{N} a_i$$
$$\Rightarrow \sum_{i=1}^{N} a_i^{p_+} \leq max\{1, N^{1-p_+}\} \left(\sum_{i=1}^{N} a_i\right)^{p_+}$$

or:

$$\sum_{i=1}^{N} a_i^{p_+} \leq c \left(\sum_{i=1}^{N} a_i\right)^{p_+}.$$

Theorem 1.4.9 (Radon measurement [32].)**.**

In what follows, E is a topological space separate assume locally compact. $C_K(E)$ is the vector space of continuous functions at values in $\mathbb{R}$ Where $\mathbb{C}$ at support included in the compact K, when it is necessary to specify it, we will write $C_K(E, \mathbb{R})$ Where $C_K(E, \mathbb{C})$.
$C_C(E)$ is the vector space of continuous functions at compact stand.
We obviously have $C_C(E) = \bigcup_K C_K(E)$, and $K(E)$ is the compact family of E and the following inclusions:

$$C_K(E) \subset C_C(E) \subset C_b(E) \subset C(E).$$

($C_b(E)$ is the space of continuous and bounded functions on E, $C(E)$is the space of continuous functions on E).

Naturally if E is compact $C_C \equiv C_b \equiv C$. A natural topology is one that is induced by the topology natural on $C_b(E)$ that is to say given by the norm of uniform convergence:

$$||\varphi||_\infty = \sup_{x \in E} |\varphi(x)|.$$

Let's remember that $C_C(E)$ is not complete for this standard, however $C_K(E)$ is a Banach.

1.5 Numerical method

In this work, digital simulation is a great tool to help design and understand many physical phenomena, in engineering for example, it has made it possible to make great progress in solid mechanics and many technological innovations. In this part we will present some definitions and properties for the Finite Element Method (See [3, 53]).

1.5.1 Finite Element Method

In order to analyze an engineering system, a mathematical model is developed to describe the system. While developing the mathematical model, some assumptions aremade for simplification. Finally, the governing mathematical expression is developed to describe the behavior of the system. The mathematical expression usually consists of differential equations and given conditions. These differential equations are usually very difficult to obtain solutions which explain the behavior of the given engineering system. With the advent of high perfor-mance computers, it has become possible to solve such differential equations. Various numerical solution techniques have been developed and applied to solve numerous en-gineering problems in order to find their approximate solutions. Especially, the finiteelement method has been one of the major numerical solution techniques. One of themajor advantages of the finite element method is that a general purpose computer program can be developed easily to analyze various kinds of problems. In particular, any complex shape of problem domain with prescribed conditions can be handled withease using the finite element method. The finite element method requires division of the problem domain into many subdomains and each subdomain is called a finite element. Therefore, the problemdomain consists of many finite element patches. The finite element method has become one of the most important and useful engineering tools for engineers and scientists. This work presents introductory andsome advanced topics of the Finite Element

Method (FEM). Finite element theories, formulations and various example programs written in MATLAB are presented. The work is written as a text work for upper level undergraduate and lower level graduate courses, as well as a reference work for engineers and scientists who want to writequick finite element analysis programs. Understanding basic program structures of the Finite Element Analysis (FEA) isan important part for better comprehension of the finite element method. MATLAB is especially convenient to write and understand finite element analysis programs because a MATLAB program manipulates matrices and vectors with ease. These algebraic operations constitute major parts of the FEA program. In addition, MATLAB has built- in graphics features to help readers visualize the numerical resultsin two- and/or three- dimensional plots. Graphical presentation of numerical data is important to interpret the finite element results. Because of these benefits, many examples of finite element analysis programs are provided in MATLAB. The work contains extensive illustrative examples of finite element analyses using MATLAB program for most problems discussed in the book. Subroutines (MATLAB functions) are provided in the ppendix and a computer diskette which contains all the subroutines and example problems is also provided.

1.5.2 Principle of the method

The finite element method of the equivalence variational problems and energetics, several methods have been developed based on one formulation or another. The choice of the space of test functions $\mathcal{V}$ has greatly contributed to the diversity of methods.

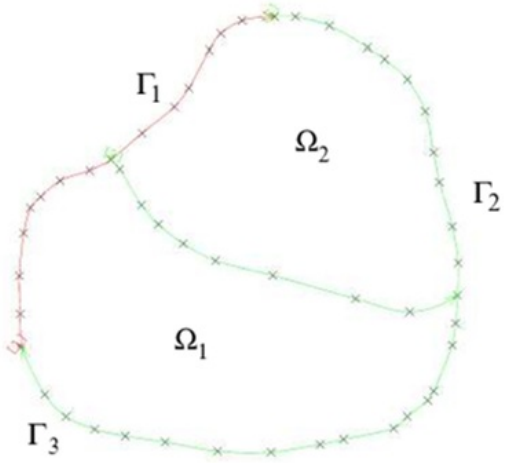

Figure 1.1: Two-dimensional domain

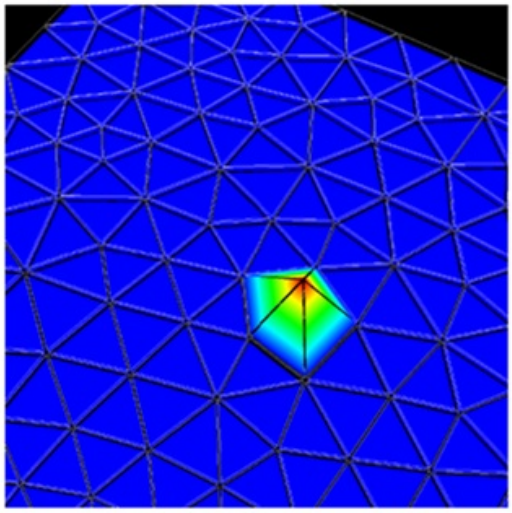

Figure 1.2: Example of triangulation

The finite element method proposes to determine the solution of the variational problem on a discretized subspace $\mathcal{V}_h$ of $\mathcal{V}$. It consists, from a differential equation, in writing the variational formulation weak of the problem. Then, to build a finite-dimensional approximation space $\mathcal{V}_h \subset \mathcal{V}$, by meshing the domain, that is to say by dividing the domain $\overline{Q} = Q \cup \partial Q$ of $\mathbb{R}^n$ into a finite number of subdomains, disjoint two by two, on which we choose a finite number of points called knots. In addition, one can choose the mode of construction of $\mathcal{V}_h$ so that the subspace $\mathcal{V}_h$ is a good approximation of $\mathcal{V}$ and that the solution u_h in $\mathcal{V}_h$ of the variational formulation is close to the exact solution u in $\mathcal{V}$. The functions of $\mathcal{V}_h$ are defined piecewise on each knots inside the domain, verify the boundary conditions at the edges of the domain and are expressed as linear combinations of simple elements (in general polynomials of degree 1, 2 or 3) called shape functions. These functions defined locally on each knot interior are continuous over the entire domain and satisfy the boundary conditions. In the case of approximation by Lagrangian elements, the first derivatives are discontinuous at the interior knots. By expressing the variational formula by the elements of $\mathcal{V}_h$ thus defined, we show that the equation transforms into a matrix system in which the unknowns are the values of the solution function at each knots. By choosing elements of simple and identical geometrical structures, the matrix processing can be systematized and carried out on a single reference element. One then proceeds to the determination of the matrixs of mass and elementary rigidity associated with an element, then one assembles these matrixs by plunging them into a single matrix representing the whole of

the field.The matrix system obtained is type, which facilitates the storage of data. Solving this system leads to the determination of the values of the solution of the initial equations in of the mesh.

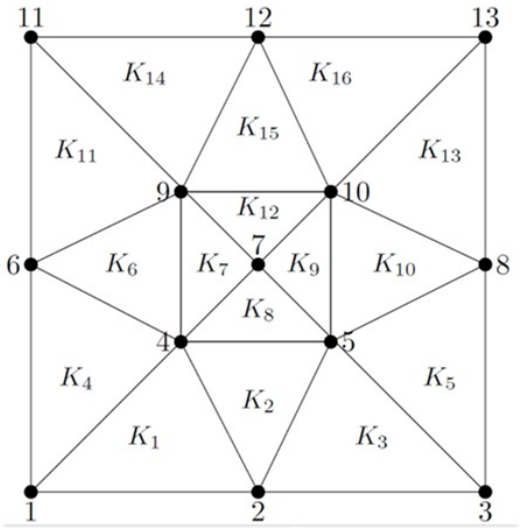

Figure 1.3: Numbering of elements and nodes

1.5.3 General internal approximation

Given a Hilbert space $\mathcal{V}$, a continuous and coercive bilinear form $a(u, w)$ and a continuous linear form $F(w)$, we consider the variational formulation: Find $u \in \mathcal{V}$ such as

$$a(u, w) = F(w) \quad \forall w \in \mathcal{V},$$

which we know has a unique solution by the Lax-Milgram theorem. the internal approximation (1.1) consists in replacing the Hilbert space $\mathcal{V}$ by a finite dimensional subspace $\mathcal{V}_h$. Trouver $u_h \in \mathcal{V}$, such as :

$$a(u_h, w_h) = F(w_h) \quad \forall w_h \in \mathcal{V}_h,$$

The resolution of the internal approximation (1.2) is easy as shown by the following lemma:

Lemma 1.5.1. *Is $\mathcal{V}$ a real Hilbert space, and $\mathcal{V}_h$ a finite dimensional subspace. Is $a(u, w)$ a continuous and coercive bilinear form on $\mathcal{V}$ and $F(w)$ a continuous linear form on $\mathcal{V}$. Then the internal approximation (1.2) admits a unique solution. Moreover, this solution can be obtained by solving a linear system with a positive definite matrix (and symmetric if $a(u, w)$ is symmetric).*

Proof. The existence and uniqueness of $\sqcap_h \in \mathcal{V}_h$,solution of (1.2) flow of the Lax-Milgram theorem applied to $\mathcal{V}_h$. To put the problem in a simpler form, we introduce a basis $(\psi_i)_{1\leq i\leq m}$ of $\mathcal{V}_h$.

so :

$$U_h = \sum_{i=1}^{m} u_i \psi_i,$$

we pose $U_h = (u_1, u_2, ..., u_m)$ the vector in $\mathbb{R}^m$ coordinates of U_h. The problem (1.2) is equivalent to find $U_h \in \mathbb{R}^m$ such as :

$$a(\sum_{i=1}^{m} u_i \psi_i, \psi_j) = F(\psi_j) \quad \forall 1 \leq j \leq m,$$

which is written in the form of a linear system:

$$\mathcal{K}_h U_h = b_h,$$

with, for $1 \leq i, j \leq m$,

$$(\mathcal{K})_{ji} = a(\psi_i, \psi_j),$$

$$(b_h)_j = F(\psi_j).$$

The coercivity of the bilinear form $a(u, w)$ results in the positive definite character of the matrix $(\mathcal{K})_h$, and therefore its reversibility. Indeed, for any vector $U_h \in \mathbb{R}^m$ we have

$$(\mathcal{K}_h U_h, U_h) \geq \nu \| \sum_{i=1}^{m} u_i \psi_i \|^2 \geq c|U_h|^2,$$

with $c > 0$, because all the standards are equivalent in finite dimension ($|.|$ denotes the Euclidean norm in $\mathbb{R}^m$). Also, the symmetry of $a(u, w)$ implies from that $(\mathcal{K})_h$ exist. □

In mechanical applications the matrix $(\mathcal{K})_h$, is called the stiffness matrix. The parameter h of $(\mathcal{V})_h$, corresponds to the maximum size of the meshes or cells which make up the mesh. Typically a base of $(\mathcal{K})_h$,will consist of functions whose support is localized on one or some meshes. This will have two important consequences: on the one hand, within the limit $h \to 0$, space $(\mathcal{V})_h$, will be bigger and will approach better the entire space $(\mathcal{V})$, and on the other hand, the stiffness matrix $(\mathcal{K})_h$, of the system will be sparse, that is to say that most of its coefficients will be zero (which will limit the cost of the numerical resolution).

Remark 1.5.2. (condition inf-sup). In the case of formulation (1.1), we have the following theorem:

Theorem 1.5.3. *That is $\mathcal{V}$, a Hilbert space, has a continuous bilinear form, F a continuous linear form. Then the problem (1.1) admits one and only one solution if and only if:*

$$\exists \alpha > 0 \quad \inf_{u \in \mathcal{V}} \sup_{w \in \mathcal{V}} \frac{a(u,w)}{\|v\|\|w\|} \geq \alpha.$$

This condition is called condition inf-sup.Unlike the Lax-Milgram theorem, this theorem provides a necessary and sufficient condition for the formulation to be well-posed:

$$\exists \alpha_h > 0 \quad \inf_{u_h \in \mathcal{V}_h} \sup_{w_h \in \mathcal{V}_h} \frac{a(u_h,w_h)}{\|v_h\|\|w_h\|} \geq \alpha_h.$$

This relation is called the discrete inf-sup condition.

Nothing guarantees a priori that the discrete inf-sup condition will be verified, even if the inf-sup condition is verified. We will now compare the error made by replacing the space $\mathcal{V}$ by its subspace $\mathcal{V}_h$. More precisely, we will increase the difference $\|u - u_h\|$ where u is the solution in $\mathcal{V}$ and u_h the one in $\mathcal{V}_h$. Let us first specify some notations: we note $\nu \geq 0$ the coercivity constant and $M$the continuity constant of the bilinear form $a(u,w)$ which verify:

$$|a(u,u)| \geq \nu \|u\|^2, \quad \forall u \in \mathcal{V},$$

$$|a(u,w)| \leq M\|u\|\|w\|, \quad \forall u,w \in \mathcal{V}.$$

The following lemma, due to Jean Céa, shows that the distance between the exact solution u and the approximate solution u_h is increased uniformly with respect to the subspace $\mathcal{V}_h$ by the distance between u and $\mathcal{V}_h$.

Lemma 1.5.4. *[44]*

We place ourselves under the hypothesis of the lemma. That is u solution of (1.1) and u_h we have :

$$\|u - u_h \leq \|\frac{M}{\nu} \inf_{w_h \in \mathcal{V}_h} \|u - w_h\|.$$

Proof. Since $\mathcal{V}_h \subset \mathcal{V}$, we deduce, by subtraction of the variational formulations (1.1), that:

$$a(u - u_h, v_h) = 0, \quad \forall v_h \in \mathcal{V}_h,$$

we choose $v_h = u_h - w_h$ we obtain :

$$\begin{aligned} \nu||u - w_h||^2 &= a(u - u_h, u - u_h) \\ &\leq a(u - u_h, u - w_h) \\ &= M||u - u_h||||u - w_h||. \end{aligned}$$

□

Finally, to demonstrate the convergence of this variational approximation, we give a last general lemma.

Lemma 1.5.5. *We place ourselves under the hypothesis of Lemma 1.3.1. We assume that there is a subspace $\widehat{\mathcal{V}}_h \subset \mathcal{V}$ dense in $\mathcal{V}$ and an app π_h of $\widehat{\mathcal{V}}_h$ in $\mathcal{V}$ such as :*

$$\lim_{h\to 0} \|v - \pi_h\| = 0, \quad \forall v \in \mathcal{V}_h.$$

Then the internal approximation method converges, that is to say:

$$\lim_{h\to 0} \|u - u_h\| = 0.$$

Proof. That is $\varepsilon > 0$, by density $\widehat{\mathcal{V}}_h$, it exists $v \in \widehat{\mathcal{V}}_h$ such as :

$$\|u - v\| \leq \varepsilon.$$

Furthermore, there exists $h_0 > 0$(depends on ε) such that, for this element $u \in \widehat{\mathcal{V}}_h$,
we have :

$$\lim_{h\to 0} \|v - \pi_h(v)\| \leq \varepsilon, \quad \forall h_0 \leq h.$$

By the lemma, we have:

$$\begin{aligned} ||u - w_h|| &\leq c\|u - \pi_h(v)\| \\ &\leq c(\|u - \pi_h(v)\| + \|v - \pi_h(v)\|) \\ &\leq 2c\varepsilon, \end{aligned}$$

from which we deduce the result. □

1.5.4 The 1D finite element method

The space we seek to approximate is:

$$\mathcal{V} = \{u \, continuous \, and \, \mathcal{C}^1 \, in \, pieces \, on \, Q = [0,1], u(0) = u(1) = 0\},$$

and we want to construct approximation spaces $\mathcal{V}_h \subset \mathcal{V}$ of finite dimension. We start by building a mesh of the interval [0, 1]:

$$0 = x_0 < x_1 < x_2 ..... < x_n < x_{n+1} = 1,$$

that is to say we divide the interval [0, 1] into small subintervals $[x_i, x_{i+1}], i = 0, ..., n$.
Intervals $[x_i, x_{i+1}], i = 0, ..., n$ are called the cells or the meshes or the elements of the mesh. We will note $h_i = x_{i+1} - x_i$ mesh size i and we define:

$$h = \max_{0 \leq i \leq n} (x_i - x_{i+1})$$

the pitch of the mesh. In the sequel, and for reasons of simplicity, we will often have to consider meshes where the points x_i are evenly spaced so that:

$$x_i = ih \; with \quad h = \frac{1}{n+1}$$

Such meshes are said to be uniform. We also define $\mathbb{P}_k$ the space of polynomials of degree less than or equal to k :

$$\mathcal{V}_h = \{p(x) = \Sigma_{i=1}^{n} a_i x^i, a_i \in \mathbb{R}\}$$

It is a vector space of dimension $k + 1$.

1.5.5 Finite element approximation $\mathbb{P}_1$

We introduce the finite dimensional functional space composed of continuous functions on Q, affines on each stitch $[x_i, x_{i+1}]$ of the mesh and null in 0 and in 1

$$\mathcal{V}_h = \{w \in \mathcal{C}^0(Q), w_{[x_i, x_{i+1}]} \in \mathbb{P}_1, w(0) = w(1) = 0, 0 \leq i \leq n\}.$$

The index of $\mathcal{V}_h$ refers to the pitch of the mesh. Space $\mathcal{V}_h$is an n-dimensional vector space since a function of $\mathcal{V}_h$ is entirely determined by the values it takes at the interior points of the mesh $w(x_i), 1 \leq i \leq n$. A basis of $\mathcal{V}_h$ is given by the functions $(\varphi_1, \varphi_2, \varphi_3, ...\varphi_n)$ continuous, affine on each element $[x_i, x_{i+1}]$ and such as:

$$\forall i \in 0, 1, ...n, \quad \forall i \in 0, 1, ...n+1, \quad \varphi_i(x_j) = \delta_{ij}$$

where δ denotes the Kronecker symbol.

Let's introduce the function $\varphi(x)$ by $\varphi(x) = \begin{cases} 1 - |x|, \text{ if } |x| \leq 1 \\ 0, \; some\, where\, else. \end{cases}$

If the mesh is uniform, then each function φ_i has the expression $\varphi_i(x) = \varphi(\frac{x - x_i}{h})$. In the base $(\varphi_1, \varphi_2, ..., \varphi_n)$, a function u belonging to $\mathcal{V}_h$ has for expression :

$$u(x) = \Sigma_{i=1}^{n} u(x_i)\varphi_i(x)$$

The whole point of the finite element method lies in the fact that each basis function φ_i has a very reduced support, that is to say that the set of x such as $\varphi_i(x) \neq 0$ is small compared to the resolution domain $Q = [0,1]$. Figure Mesh of Q = [0, 1] and basis function in finite element $\mathbb{P}_1$. This has the consequence that most of the coefficients of the stiffness matrix $A_{ij} = a(\varphi_j, \varphi_i), 1 \leq i, j \leq n$ are zero. Indeed, we illustrate the method on the simple example of the Poisson problem $1D$:

$$\begin{cases} -\partial^2_{x^2} u = f, \text{ in } Q \\ 0, \text{ on } \partial Q. \end{cases}$$

$$A_{ij} = a(\varphi_j, \varphi_i) = \int_0^1 \partial_x \varphi_j(x) \partial_x \varphi_i(x) dx$$

and if j is not equal to $i-1, i$ Where $i+1$, then the functions φ_i, φ_{i-1} et φ_{i+1} have disjoint supports and the integral in (1.15) is zero. The non-zero coefficients are easily calculated

$$A_{i-1,i} = a(\varphi_{i-1}, \varphi_i) = \int_0^1 \partial_x \varphi_{i-1}(x) \partial_x \varphi_i(x) dx = \int_{x_{i-1}}^{x_i} -\frac{1}{h}\frac{1}{h} dx = -\frac{1}{h},$$

$$A_{i,i} = a(\varphi_i, \varphi_i) = \int_0^1 (\partial_x \varphi_i(x))^2 dx = \int_{x_{i-1}}^{x_i} \frac{1}{h^2} dx + \int_{x_i}^{x_{i+1}} \frac{1}{(-h)^2} dx = \frac{2}{h},$$

$$A_{i+1,i} = a(\varphi_{i+1}, \varphi_i) = \int_0^1 \partial_x \varphi_{i+1}(x) \partial_x \varphi_i(x) dx = \int_{x_{i+1}}^{x_i} \frac{1}{h}\frac{-1}{h} dx = -\frac{1}{h}.$$

Finally, the stiffness matrix is a tridiagonal matrix:

$$\mathrm{A} = \frac{1}{h} \begin{bmatrix} 2 & -1 & 0 & 0.....0 & 0 & 0 \\ -1 & 2 & -1 & 0.....0 & 0 & 0 \\ 0 & 0 & 0 & 0.....0 & 0.. & 0 \\ 0 & 0 & 0 & 0.....0 & 0.. & 0 \\ 0 & 0 & 0 & 0.....0 & 0.. & 0 \\ 0 & 0 & 0 & 0..... -1 & 2 & -1 \\ 0 & 0 & 0 & 0.....0 & -1 & 2 \end{bmatrix}$$

The following proposition shows that the matrix A is invertible:

Theorem 1.5.6. *The matrix A is positive definite that is to say it satisfies the following property, $\forall U \in \mathbb{R}^n - \{0\}, \quad (AU, u) > 0$. Before giving the proof of this proposition, let us explain why it implies the invertibility of the matrix A. Indeed, if A is not invertible, then there*

is a vector $U \neq 0$ in $\mathbb{R}^n$ such as $AU = 0$. This implies in particular that $(AU, U) = 0$ with $U \neq 0$, which contradicts the fact that A is positive definite.

Proof. That is $U = (u_1, ..., u_n) \neq 0$ in $\mathbb{R}^n$.The vector AU has for coordinates:

$$(\sum_{i=1}^{m} A_{1j}u_j, ...A_{nj}u_j) = (\sum_{i=1}^{m} a(\varphi_j, \varphi_1)u_j, ..., \sum_{i=1}^{m} a(\varphi_j, \varphi_n)u_j)$$

$$(AU, U) = \sum_{j=1}^{n}\sum_{i=1}^{n} a(\varphi_j, \varphi_i)u_j u_i = a(\sum_{i=1}^{m}\varphi_j u_j, \sum_{i=1}^{m}\varphi_i u_i) = a(u_h, u_h) = \int_0^1 |\partial_x u_h(x))|^2 dx,$$

where $u_h(x)$ is the function of $\mathcal{V}_h$ defined by $u_h(x) = \sum_{j=1}^{n} u_j\varphi_j(x)$. Like the $(u_1, ..., u_n)$ are not all zero, it is easy to verify that $u_h(x)$ is not zero, which implies that $\int_0^1 |\partial_x u_h(x))|^2 dx > 0$. □

To get the second member $F = (f, \varphi_i) \quad i = 1, ..., n$, you have to calculate the integrals: $\int_0^1 f(x)\varphi_i(x) = \int_{x_{i-1}}^{x_i} f(x)\varphi_i(x) + \int_{x_i}^{x_{i+1}} f(x)\varphi_i(x)$ in general, this integral cannot be calculated exactly because the function f can be complicated. In practice, we use numerical integration techniques where, on each interval $[x_i, x_{i+1}]$, we approximate the integral by a quadrature formula.

1.5.6 Finite element approximation $\mathbb{P}_2$

In certain applications, one can consider that the approximation by straight lines on each element of the mesh $[x_i, x_{i+1}]$, is too coarse, that is to say that it provides an approximate function too far from the exact function u. We can then try to approximate u on each mesh by polynomials of higher degree. The finite element approximation $\mathbb{P}_2$ consists in approximating the solution u by a continuous function on Q, and polynomial of degree 2 on each mesh $[x_i, x_{i+1}]$. The approximation space is then defined by:

$$H_h = \{v \in \mathcal{C}^0(Q), v_{[x_i, x_{i+1}]} \in \mathbb{P}_2, v(0) = v(1) = 0, 0 \leq i \leq n\}.$$

Noting,

$$x_{i+\frac{1}{2}} = \frac{x_i + x_{i+1}}{2},\ i = 0, 1, 2, ...n,$$

the centers of the cells, we see that any function of H_h is entirely determined by the data of the values it takes at the interior points of the mesh $x_i, i = 1, ...n$, as well as at the points $x_{i+\frac{1}{2}}, i = 1, ...n$. The vector space H_h is therefore of dimension $2n + 1$. A basis of H_h is given by the functions $\psi_i, i = 1, ...n$ such that :

$$\psi_i \in H_h, \psi_i(x_j) = \delta_{ij}, \psi_i(x_{j+\frac{1}{2}}) = 0, \forall j$$

and by the functions $\psi_{i+\frac{1}{2}}(x); i = 0, ...n$ as :

$$\psi_{i+\frac{1}{2}} \in H_h, \psi_{i+\frac{1}{2}}(x_j) = 0, \psi_i(x_{j+\frac{1}{2}}) = \delta_{ij}, \forall j.$$

We also define two functions which allow to give the expressions of the basic functions:

$$\text{the function by } \varphi(x) = \begin{cases} (1+x)(1+2x), \text{ if } -1 \leq x \leq 0 \\ (1-x)(1-2x), \text{ if } 0 \leq x \leq 1 \\ 0, \ elsewhere, \end{cases}$$

and

$$\text{the function by } \psi(x) = \begin{cases} 1-4x^2, \text{ if } x \leq \frac{1}{2} \\ (1-x)(1-2x), \text{ if } x > \frac{1}{2} \end{cases}$$

if the mesh is uniform, then $\psi_i = \varphi(\frac{x-x_i}{h})$ and $\psi_{i+\frac{1}{2}} = \varphi(\frac{x-x_{i+\frac{1}{2}}}{h})$ in two dimensions, we always illustrate the finite element method on the case of the Poisson problem:

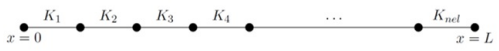

Figure 1.4: Mesh in dimension 1

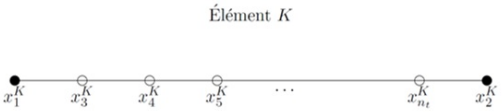

Figure 1.5: Geometric nodes and calculation of the element K

$$\begin{cases} -div\nabla \cdot u = f, \text{ in } Q \\ u = 0, \text{ on } \partial Q \end{cases}$$

where this time Q is a bounded open set of $\mathbb{R}^2$. We assume that the variational formulation of this problem admits a solution u in the space $\mathcal{V}$:

$$\mathcal{V} = \{u \, continuous \, and \, \mathcal{C}^1 \, in \, pieces \, on \, Q = [0,1], u(0) = u(1) = 0, \}$$

$$\mathcal{V} = \{u \, continuous \, and \, \mathcal{C}^1 \, in \, pieces \, on \, \overline{Q}, u = 0, \, on \, \partial Q\}$$

and we try to approximate it by a function u_h solution of the same variational problem but where the space $\mathcal{V}$ is replaced by an approximation space $\mathcal{V}_h$. We Start by defining what is a mesh of the domain Q in dimension two.

Definition 1.5.7. A triangular mesh of the domain Q is a set τ_h of unflattened triangle $(K_i)_{1\leq i\leq n}$ which subdivide the domain Q. By convention, the parameter h designates the length of the largest edge of the mesh. We assume that the triangles do not overlap and that the intersection between two triangles K_i and K_j is either empty, or equal to a vertex common to the two triangles, or to an edge common to the two triangles. two triangles. In addition, one calls vertices or nodes of the mesh the vertices of the triangles making up the mesh.

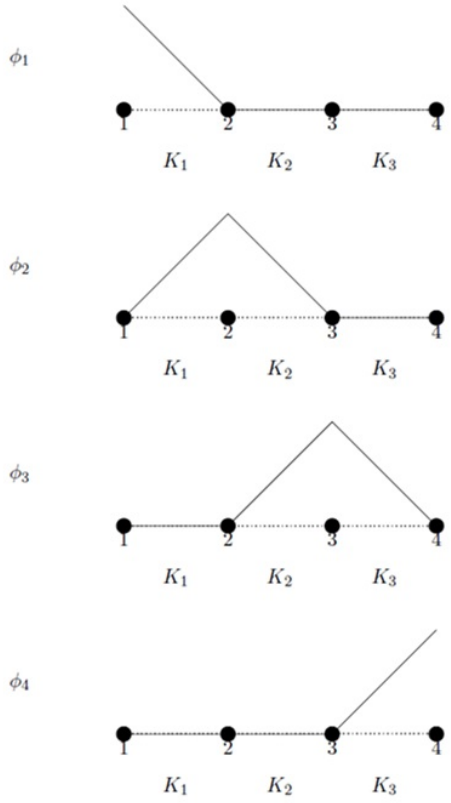

Figure 1.6: φ Linear Functions by Element

Remark 1.5.8. We consider here a subdivision of the domain Q into triangles, but we could also build meshes composed of quadrilaterals or generally by polygons. As in dimension one, we define $\mathbb{P}_k$ the space of polynomials of two variables of degree less than or equal to k:

$$\mathbb{P}_k = \{p(x,y) = \Sigma_{i+j\leq k} a_{ij} x^i y^j, a_{ij} \in \mathbb{R}\}.$$

For example, a polynomial of degree one is written generically $p(x, y) = a + bx + cy$, while a polynomial of degree two is written $p(x, y) = a + bx + cy + dxy + tx^2 + ly^2$. The approximation spaces $\mathcal{V}_h$ are defined in the same way as in dimension one, by choosing functions which are globally continuous on Q and which are polynomial on each triangle K_i of the mesh. For the approximation $\mathbb{P}_1$ for example, we have:

$$\mathcal{V}_h = \{u \in \mathcal{C}^0(Q), u_k \forall k_i \in \tau_h, \, et \, u = 0 \, \text{on} \, \partial Q\}.$$

This space admits as basic functions, the hat functions φ_i which take the value 1 at a node (x_i, y_i) of the mesh and the value 0 at the other nodes (x_j, y_j) of the mesh.
The stiffness matrix is calculated as for dimension one by the formula :

$$A_{ij} = a(\varphi_j, \varphi_i) = \int_Q \nabla \cdot \varphi_j(x, y) \nabla \cdot \varphi_i(x, y) dxdy,$$

and the second member:

$$(f, \varphi_i) = \int_Q f(x, y) \varphi_i(x, y) dxdy,$$

is calculated in an approximate way by quadrature formulas.

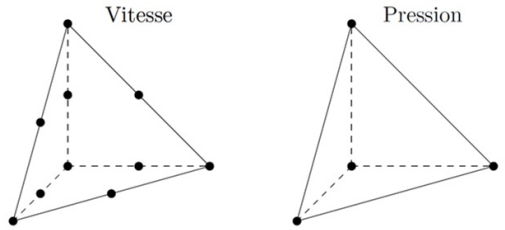

Figure 1.7: Tetrahedral reference element with 4 and 10 nodes

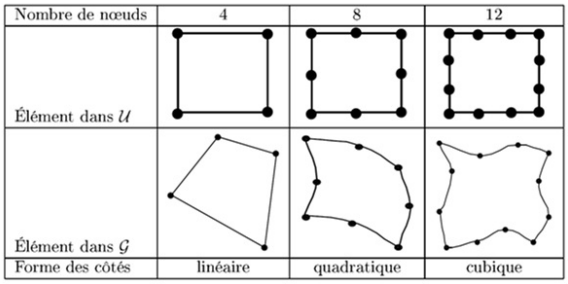

Figure 1.8: 4 Linear, 8 Quadratique, 12 Cubic

1.5.7 Convergence of the finite element method

We assume here that we are solving a problem on a domain $Q \in \mathbb{R}^n$ in a way approached by the finite element method. The purpose of this section is to provide an estimate of the error $\|u - u_h\|_m$ where $\|.\|$ denotes the norm H^m. The regularity of u and of u_h (and therefore the possible values for m) obviously depending on the continuous problem and the type of finite elements chosen for its resolution, we will expose here the approach in a general way, by supposing the sufficiently regular functions compared to the value of m. In practice, we will most often have $m = 0, 1$ where 2. We will note τ_h the mesh of $Q \in \mathbb{R}^n$ considered. We assume here the domain Q polygonal, which allows to cover exactly by the mesh. If this is not the case, the calculations which follow must be modified to take account of the difference between the domain covered by the mesh and the real domain. The different stages of the calculation will be, quite schematically, as follows:

1- The approximation error is bounded by the interpolation error:

$$\|u - u_h\|_m \leq C\|u - \pi_h u\|_m.$$

2- We are reduced to local increases on each element:

$$\|u - \pi_h u\|_m^2 = \sum_{k \in \tau_h} \|u - \pi_h u\|_{m,k}^2.$$

3- We come back to the reference element:

$$\|u - \pi_h u\|_{m,k}^2 \leq C(k)\|\widehat{u} - \widehat{\pi}_h \widehat{u}\|_{m,\widehat{k}}^2.$$

4- Increases on the reference element:

$$\|\widehat{u} - \widehat{\pi}_h \widehat{u}\|_{m,\widehat{k}}^2 \leq C_1 \|\widehat{u}\|_{k+1,\widehat{k}}^2.$$

5- Assembly of local increases:

$$\|u - \pi_h u\|_m \leq C h^{k+1-m} \|u\|_{k+1}.$$

1.5.8 Mark-up by interpolation error

The equation of the lemma indicates that :

$$\|u - u_h\|_m \leq \frac{M}{\nu} \|u - w_h\|_m, \quad \forall w_h \in \mathcal{V}_h.$$

It can be applied in the special case where $w_h = \pi_h u$,Which give:

$$\|u - u_h\|_m \leq \frac{M}{\nu}\|u - \pi_h u\|_m.$$

1.5.9 Decomposition on elements

We have, with obvious notations:

$$\begin{aligned} ||u - \pi_h u||_m^2 &= \sum_{k\in\tau_h} \|u - \pi_h u\|_{m,k}^2 \\ &= \sum_{k\in\tau_h}\sum_{i=0}^{m} \|u - \pi_h u\|_{i,k}^2, \end{aligned}$$

the calculation is thus reduced to a calculation on each element, for all the semi-norms $|.|_{i,k}, i = 0, ..., m$.

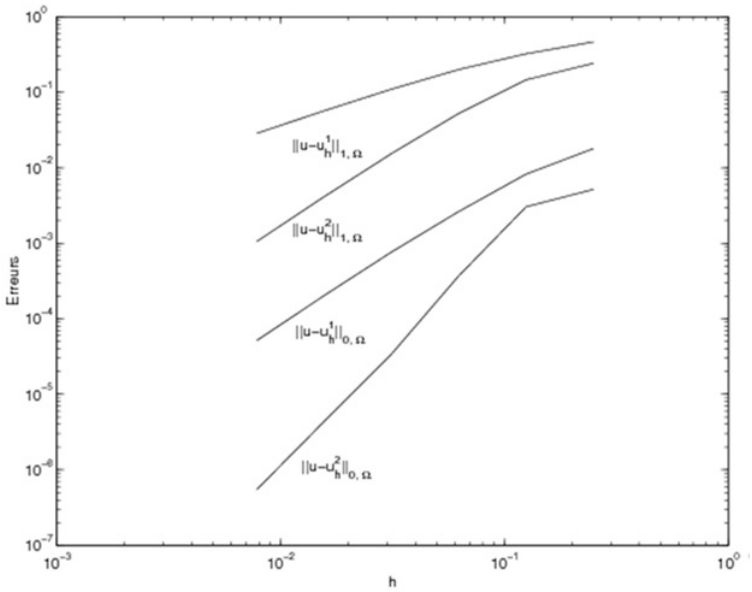

Figure 1.9: Errors made for linear and quadratic approximations

1.5.10 Switch to reference element

Theorem 1.5.9. *Either K any element of τ_h, and $\widehat{k}$ the reference element. That is G the affine transformation of $\widehat{k}$ towards $K : G(\widehat{x}) = B\widehat{x} + b$, with B invertible.*

Chapter 2

Deformation of beams geometry

Figure 2.1: A simplified schematic diagram of some geometric shapes(1)

Figure 2.2: A simplified schematic diagram of some geometric shapes(2)

Due to impressive effects of thermal loads on the behavior of structures, especially plates and shells, it is required to analyze these structures in thermal environment. Extensive researches were presented about thermal analysis of shells. Some books were published in this area [8-10]. However, there are few studies on the nonlinear behavior of these structures under the both mechanical and thermal loads. So the topic still attracts the researchers view. Furthermore, geometrically nonlinear behavior of shells in thermal environment is also unknown. Therefore, using a finite element procedure which can be used to thermomechanical nonlinear analysis of shells may be applicable to identify the large deffections of general shell structures under both thermal and mechanical loads. Figure (2).

2.1 Geometrical analysis of the beam

2.1.1 Bresse beam model

The third edition of the work Vibration Problems in Engineering, written by Timoshenko in 1955, in collaboration with D.H. Young, again, mentions Lord Rayleigh's [42] contribution to the accounting of rotary inertia. Authors refrain from mentioning Bresse's [19] work although the book, by Timoshenko and Young published in 1955, was published after Timoshenko's 1953 [49] (p.151) work on the history of strength of materials. This is where Timoshenko specifically mentioned that Bresse [50] was the first investigator who introduced the rotary inertia.

The Bresse system [19] is known as the circular arch problem and composed of three coupled wave equations given by

$$\begin{cases} \rho_1\varphi_{tt} = Q_x + lN + F_1, \\ \rho_2\psi_{tt} = M_x - Q + F_2, \\ \rho_3\omega_{tt} = N_x - lQ + F_3, \end{cases} \tag{2.1}$$

where φ, ψ and ω denote, respectively, the vertical, shear angle and longitudinal displacements. By $F_i, i = 1, 2, 3$ we are denoting external forces. We use N, Q and M to denote the axial force, the shear force and the bending moment which take the following form

$$N = k_0(\omega_x - l\varphi), Q = k(\varphi_x + l\omega + \psi), M = b\psi_x.$$

The coefficients of the system are given by

$$\rho_1 = \rho A,\ \rho_2 = \rho l,\ k_0 = EA,\ k = k'GA,\ b = El,\ l = R^{-1}$$

such that ρ, E, G, k, A, l and R represent, respectively, the density of material, the modulus of elasticity, the shear modulus, the shear factor, the cross-sectional area, the second moment of area of the cross-section and the radius of curvature. We assume that all these quantities are positives, we refer the reader to (see for [24],[34],[52]).

2.1.2 Timoshenko beam

The use of the Google Scholar produces about 78,000 hits on the term Timoshenko beam. The question of priority is of great importance for this celebrated theory. For the first time in the world literature, this study is devoted to the question of priority. It is that Stephen

Prokofievich Timoshenko had a co-author, Paul Ehrenfest. It so happened that the scientific work of Timoshenko dealing with the effect of rotary inertia and shear deformation does not carry the name of Ehrenfest as the co-author. In his 2002 book, Grigolyuk concluded that the theory belonged to both Timoshenko and Ehrenfest. This work confirms Grigolyuk's discovery, in his little known biographic work about Timoshenko, and provides details, including the newly discovered letter of Timoshenko to Ehrenfest, which is published here for the first time over a century after it was sent. This thesis establishes that the beam theory that incorporates both the rotary inertia and shear deformation as is known presently, with shear correction factor included, should be referred to as the Timoshenko- Ehrenfest beam theory.

In 1921, Timoshenko [48] considered the system

$$\begin{cases} \rho u_{tt} = k\left(u_x + \varphi\right)_x, \\ I_\rho \varphi_{tt} = \left(EI\varphi_x\right)_x + k\left(u_x - \varphi\right). \end{cases} \tag{2.2}$$

As a simple model describing the transverse vibration of a beam. Where u is the transverse displacement of the beam and φ is the rotation angle of the filament. The coefficients ρ, I_ρ, E, I and k are respectively the density (the mass per unit length), the polar moment of inertia of a cross section,Young's modulus of elasticity, the moment of inertia of a cross section and the shear modulus. In recent years, the problem of existence and stability of the Timoshenko system, hyperbolic nonlinear term and second sound has attracted a considerable attention to a lot of mathematicians. Many results have been established concerning existence and asymptotic behavior. (see for [5],[11],[12],[29],[30],[33],[38]). It should be noticed that mentioned problem plays a crucial role in ingineering applications and for more details on the resourches valuable that has been realised regardiing Timoshenko systems, we refer the readers to (see for [12], [13], [14], [15], [16], [39]).

2.1.3 Euler-Bernoulli beam

Due to the nature of beams in structural engineering, it is more convenient to investigate a single spanned, prismatic constant cross sectional homogenous beam in Cartesian righthanded 3D- coordinate axes system, such that, the positive x is left to right direction and positive y is directed toward the viewer and positive z is in a downward direction. All terminologies and signed quantities in whole of this thesis will be referenced to this coordinate system which is also

the most used one in analytical and numerical plate theories and in finite element methods. Moreover, in order to clarify the basic fundamentals of such beam analysis, it is better to consider as an illustrative entrance, the real deflection curve for a built-in beam subjected to uniform load as shown in Fig.(2.3), in which two inflection points divided the beam into three parts. The outer parts concaved- down while the middle part concaved- up. Points 1,2,3 and 4 are general points at which the perpendiculars to the tangents (that is to say, normals) are shown. These portions are rearranged as shown in Fig.(2.3) for mathematical purposes. This deflection curve was obtained based on kinematical assumptions due to Euler Bernoulli-Navier hypothesis, which in turn leads to the well-known Euler-Bemoulli Beam Theory (EBBT). The relevant basic data and relations concerned with Euler-Bemoulli Beam EBB. The most often used sign convention in main textbooks for analysis quantities such as shown in Fig. (2.3), as well as the mathematical definition of positive orientation of surfaces were followed in this work.

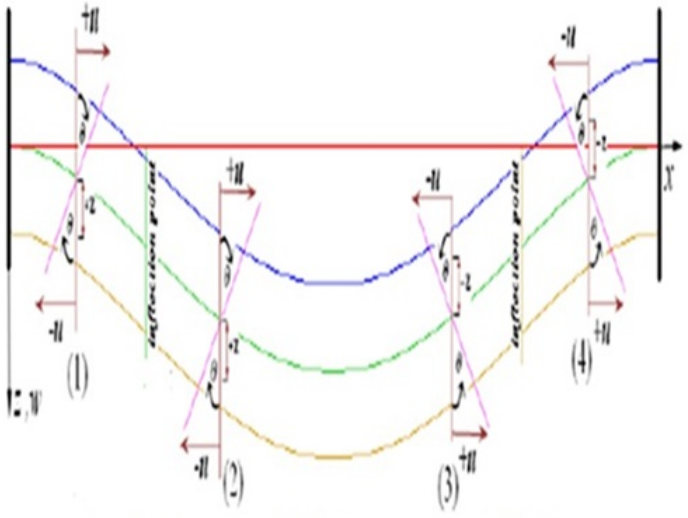

Figure 2.3: Exaggerated deflection curve for a built-in beam.

In case of pure shear, the angle between each of tangents to each of these warped curves and their corresponding initial normal is equal to the shearing strain γ provided that its maximum value occurs at neutral axis as natural consequence of shearing stress distribution effect, which in turn was assigned by Timoshenko for the whole of each section although it must vary in the same manner as shearing stress. Consequently, this theory relaxes the Bernoulli-Navier

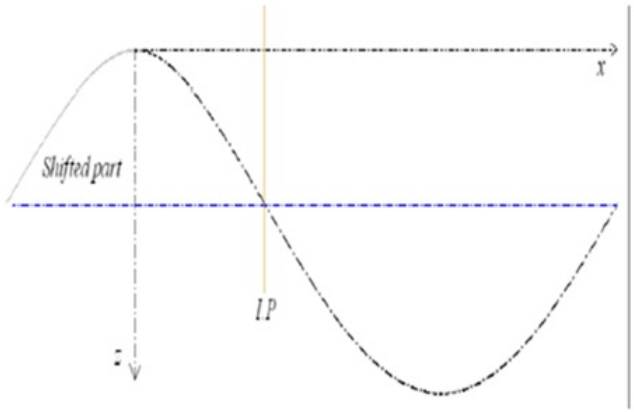

Figure 2.4: Concaved- up and concaved-down portions.

normality hypothesis, but at the same time neglects the warpage shape of originally plane cross section, therefore this assumed constant shearing strain through the beam thickness should correspond to a constant shearing stress max.

2.1.4 Euler-Bernoulli Hypothesis

In this section reference is often made to the beam axis. The meaning of the beam axis is intuitive for a prismatic beam with a rectangular cross-section. It is the middle axis. Other terms, such as: neutral axis, bending axis and centroidal axis are also frequently used. They all express the same property that no axial stresses σ_{xx} should develop on the axis under pure bending.

Hypothesis 1: Plan Remains Plane

This is illustrated in Figure (3.55) showing an arbitrary cross-section of the beam before and after deformation. Imagine a straight cut made through the undeformed beam. The plane-remains-plane hypothesis means that all material points on the original cut align also on a plane in the deformed beam. The cases (b) and (c) obey the hypothesis but the warped section (d) violates it.

Hypothesis 2: Normal Remains Normal

If the initial cut were made at right angle of the undeformed beam axis as in Figure ((2.6) (a)), it should remain normal to the deformed axis, see Figure ((2.6)(b)). In the sketch on Figure (2.6) (c) the hypothesis is violated when the angle $\alpha \neq 90°$. The Euler-Bernoulli hypothesis

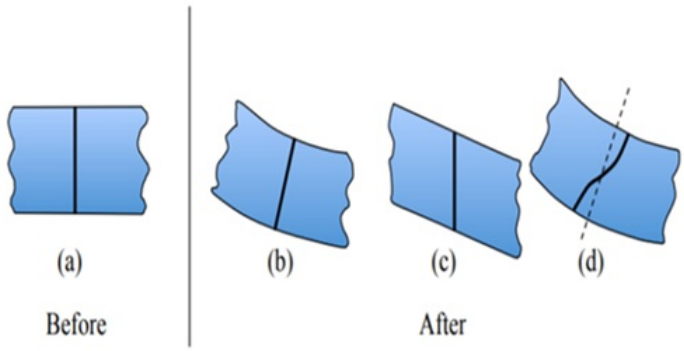

Figure 2.5: Flat (b) and (c) and warped (d) cross-sections after deformations.

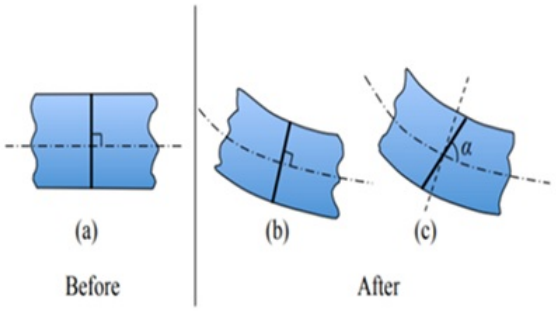

Figure 2.6: Testing the normal-remains-normal hypothesis.

gives rise to an elegant theory of infinitesimal strains in beams with arbitrary cross-sections and loading in two out-of-plane directions. The interested reader is referred to several monographs with a detailed treatment of the subject, of bi-axial loading of beams. The present set of notes on beams is developed under the assumption of planar deformation. This means that the beam axis motion is restricted only to one plane.

Mathematically, the Hypothesis 1 is satisfied when the u-component of the displacement vector is a linear function of z

$$u(z) = u^{\circ} - \theta z \quad \text{at any } x. \tag{2.3}$$

The constant first term, u° is the displacement of the beam axis (due to axial force). The second term is due to bending alone, Figure (2.7). The second Euler-Bernoulli hypothesis is satisfied if the rotation of the deformed cros section θ is equal to the local slope of the bent middle axis $\frac{dw}{dx}$

$$\theta = \frac{dw}{dx}. \tag{2.4}$$

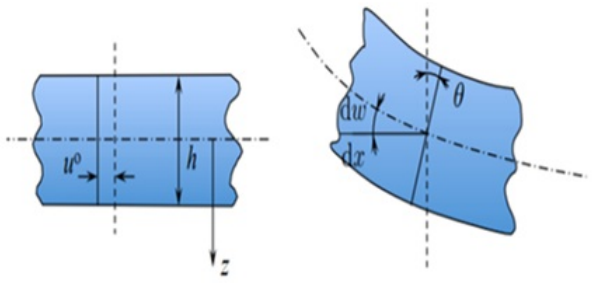

Figure 2.7: Linear displacement field through the thickness of the beams.

Eliminating the rotation angle é between equations (2.3) and (2.4) yields

$$u(x,z) = u^{\circ} - \frac{dw}{dx}z \quad \text{at any } x. \tag{2.5}$$

It can be seen from Figure (2.7) that the displacement at the bottom (tensile) side of the beam is negative, which explains the minus sign in the second term of Equations(2.4)and (2.5).

Hypothesis 3

The cross-sectional shape and size of the beam remain unchanged. This means that the vertical component of the displacement vector does not depend on the z-coordinate. All points of the cross-section move by the same amount

$$\omega = \omega(x). \tag{2.6}$$

In the case of planar deformation, which covers most of the practical cases of the beam response, the y-component of the displacement vector vanishes

$$v = 0. \tag{2.7}$$

We are now in the position to calculate all components of the strain tensor from Equation.

We are now in the position to calculate all components of the strain tensor from equation

$$\epsilon_{xx} = \frac{du_x}{dx} = \frac{du}{dx} \tag{2.8}$$

$$\epsilon_{zz} = \frac{du_y}{dy} = \frac{dv}{dy} = 0 \tag{2.9}$$

$$\epsilon_{zz} = \frac{du_{zz}}{dz} = \frac{d\omega(x)}{dz} = 0 \tag{2.10}$$

$$\epsilon_{xy} = \frac{1}{2}\left(\frac{du_x}{dy} + \frac{du_y}{dx}\right) = 0 \tag{2.11}$$

$$\epsilon_{yz} = \frac{1}{2}\left(\frac{du_y}{dz} + \frac{du_z}{dy}\right) = \frac{1}{2}\left(\frac{dv}{dz} + \frac{d\omega}{dy}\right) = 0 \tag{2.12}$$

$$\epsilon_{zx} = \frac{1}{2}\left(\frac{du_z}{dx} + \frac{du_x}{dz}\right) = \frac{1}{2}\left(\frac{d\omega}{dx} + \frac{du}{dz}\right) = \frac{1}{2}\left(\frac{d\omega}{dx} - \frac{d\omega}{dx}\right) = 0. \tag{2.13}$$

It is seen that all components of the strain tensor vanish except the one in the direction of beam axis.

Note that ϵ_{xx} is the only component of the strain tensor in the elementary beam theory. Therefore the subscript xx can be dropped and, unless specified otherwise $\epsilon_{xx} = \epsilon$ Introducing Equation (2.5) into Equation (2.6) one gets

$$\epsilon(x,z) = \frac{du^{\circ}(x)}{dx} - \frac{d^2\omega(x)}{dx^2}z. \tag{2.14}$$

The first term represents the strain arising from a uniform extension of the entire cross-section

$$\epsilon^{\circ}(x) = \frac{du^{\circ}(x)}{dx}. \tag{2.15}$$

The second term adds a contribution of bending. Introducing the definition of the curvature of the beam axis

$$k = -\frac{d^2\omega(x)}{dx^2}z \tag{2.16}$$

the expression for strain can be put in the final form:

$$\epsilon(x,z) = \epsilon^{\circ}(x) + kz. \tag{2.17}$$

Mathematically, the curvature is defined as a gradient of the slope of a curve. The minus sign in equation follows from the rigorous description of the curvature of a line in the assumed coordinate system. Physically, it assumes that strains on the tensile side of the beam are positive. A quite different interpretation of the Euler-Bernoulli hypothesis is offered by considering a two-term expansion of the exact strain profile in the Taylor series around the point

$$\epsilon(x,z) = \epsilon(x,0) + \frac{d\epsilon(x,0)}{dx}z + \frac{1}{2}\frac{d^2\epsilon(x,0)}{dx^2}z^2 + ...$$

Taking only the first two terms is a good engineering approximation but leads to some internal inconsistencies of the elementary beam theory. These inconsistencies will be explained in the two subsequent chapters.

2.1.5 Difference between Timoshenko and Euler- Bernoulli beam

As shown in Figure (2.8), difference between Timoshenko Beam and Euler Bernoulli beam model can be visibly explained. In Euler Bernoulli beam, deformation of a section $\frac{dv}{dx}$ is rotation due to bending. In Timoshenko beam theorem, deformation is summation of bending and shear deformation as shown in $\frac{dv}{dx}$ is bending and $\frac{dv}{dx}$ is shear deformation. We want to study about the transverse shear strain effect. It is shown that shear strain is constant for a particular cross- section throughout the beam and it is not distorted after the deformation. Timoshenko beam element models are not good in capturing normal stress. For capturing shear deformation, classical beam theory elements are not correct. An Euler Bernoulli beam element gives excellent results for normal stress since they are constraining the predominant bending deformation. For thin beam purpose, classical beam theory is good and for thick beam usage Timoshenko beam theory is good. Structural analysis and harmonic analysis are used to predict the stability of the beam. Equivalent stress distribution and Shear, formation along the beam are the main output parameters for the structural analysis. In addition to above mentioned methods, buckling analysis can also be used to predict the stability of the beam.

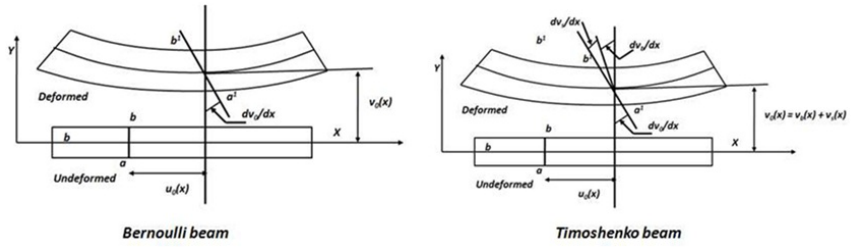

Figure 2.8: Difference between Timoshenko and Euler Bernoulli beam model

2.2 Deformation of the beam

The main objective of this work is to analyze the complex composite beams. The geometrically non-linear analysis of composite beam exhibits specific difficulties due to the anisotropic ma-

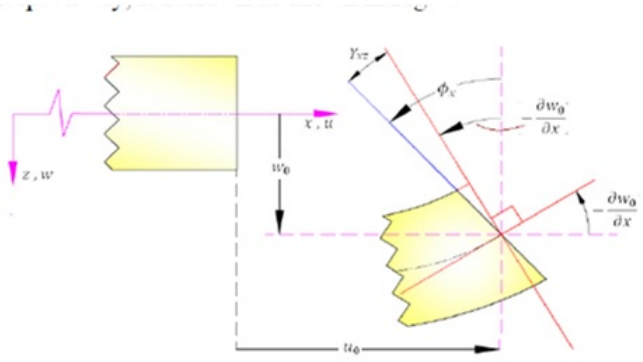

Figure 2.9: Deformation of cross section described by Reddy.

terial behavior, and to the higher non-linearity induced by a higher stiffness, inducing tensile mid-plane forces in beam higher, than that observed with conventional homogeneous materials. These structures with complex boundary conditions, loadings and shapes are not easily amenable to analytical solutions and hence one has to resort to numerical methods such as finite elements. A considerable amount of effort has gone into the development of simple beam bending elements based on the Timoshenko Beam Theory for homogeneous isotropic beam. The advantages of this approach are:

(i) it accounts for transverse shear deformation,

(ii) it requires only c0 continuity of the field variables,

(iii) it requires refined equivalent single-layer theory,

(iv) it is possible to develop finite elements based on 6 engineering degrees of freedom viz, 3 translations and 3 rotations.

However, the low- order elements, that is to say the 3-node triangular,
4-node and 8-node quadrilateral elements, locked and exhibited violent stress oscillations. Unfortunately, this element which is having the shear strain becomes very stiff when used to model thin structures, resulting inexact solutions. This effect is termed as shear-locking which makes this otherwise successful element unsuitable. Many techniques have been tried to overcome this, with varying degrees of success. The most prevalent technique to avoid shear locking for such elements is a reduced or selective integration scheme. In all these studies shear stresses at nodes are inaccurate and need to be sampled at certain optimal points derived from considerations based on the employed integration order. The use of the same interpolation functions for transverse displacement and section rotations in these elements results in a mismatch of the

order of polynomial for the transverse shear strain field. This mismatch in the order of polynomials is responsible for shear. The Euler-Bernoulli beam theory neglects shear deformations by assuming that plane sections remain plane and perpendicular to the neutral axis during bending. As a result, shear strains and stresses are removed from the theory. Shear forces are only recovered later by equilibrium $V = \frac{dM}{dx}$. In reality, the beam cross-section deforms somewhat like what is shown in Figure (2.9). This is particularly the case for deep beam, that is to say, those with relatively high cross-sections compared with the beam length, when they are subjected to significant shear forces. Usually the shear stresses are highest around the neutral axis, which is where, consequently, the largest shear deformation takes place. Hence, the actual cross-section curves. Instead of modeling this curved shape of the cross-section, the Timoshenko beam theory retains the assumption that the cross-section remains plane during bending. However, the assumption that it must remain perpendicular to the neutral axis is relaxed. In other words, the Timoshenko beam theory is based on the shear deformation mode in Figure (2.10), (2.11), (2.12), (2.14). Various boundary conditions have been considered. The effect of variations in some material and/or geometric properties of the beam have also been studied.

The deformed beam is also shown in Fig.(2.12) based on the last $W(x)$ and different sections

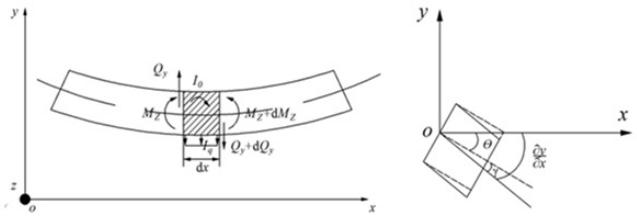

Figure 2.10: Deformation in Timoshenko Beam

deduced by Timoshenko $U(x)$- function. The deformation of elements of Timoshenko beam undergoes a rotation ϕ of the beam cross- section due to bending, in which as will be seen later in illustrative examples this rotation is independent of shear effect for all statically determinate beams and also all indeterminate beams having full symmetric conditions whereas except these beam-types, this rotation will depend on shear stiffness KGA. The bending moment M will behave in the same way. Therefore, the rotation ϕ in general will not be the same as in the Euler-Bernoulli beam. That is, $\phi \neq \theta = \frac{dW(x)}{dx}$. Moreover, the deformation of such elements also undergoes an additional angular rotation φ caused by shear. Thereby the total rotation of

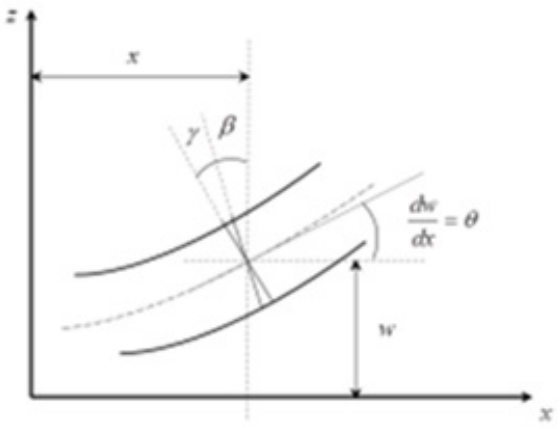

Figure 2.11: Deformation in Timoshenko Beam element

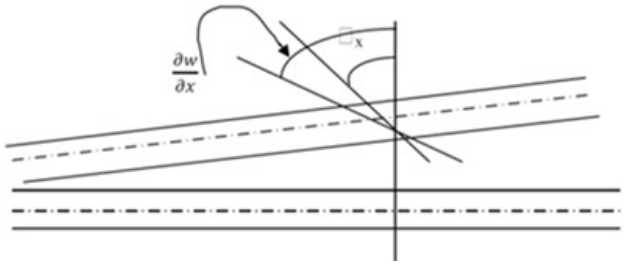

Figure 2.12: Deformation in Timoshenko Beam element

the Normal is the slope of the deflection curve W^T that is, $\frac{dW^T(x)}{dx}$ and numerically is equal the sum of these two rotations as $\frac{dW^T(x)}{dx} = (\phi + \varphi)$, where the superscripts E and T refer to Euler and Timoshenko theories respectively, is redrawn as shown in Fig(2.9).

A Timoshenko beam takes into account shear deformation and rotational inertia effects, making it suitable for describing the behavior of short beams, sandwich composite beams or beams subject to high-frequency excitation when the wavelength approaches the thickness of the beam. The resulting equation is of 4th order, but unlike ordinary beam theory - that is to say Bernoulli-Euler theory. In static Timoshenko beam theory without axial effects, the displacements of the beam are assumed to be given by

$$u_x(x, y, z) = -z\varphi(x), u_y = 0, u_z = w(x).$$

Where (x, y, z) are the coordinates of a point in the beam, u_x, u_y, u_z are the components of the displacement vector in the three coordinate directions, φ is the angle of rotation of the normal to the mid- surface of the beam and ω is the displacement of the mid- surface in z- direction.

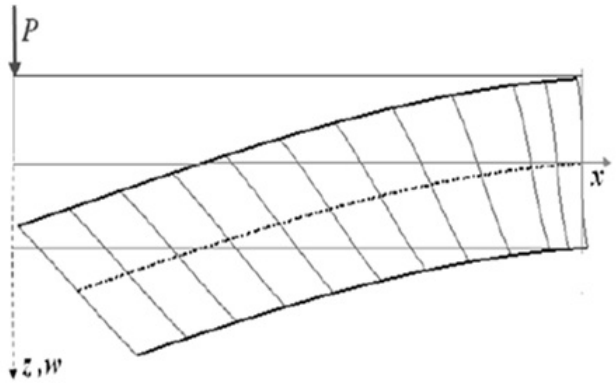

Figure 2.13: Deformed cantilever beam (warped cross sections).

The governing equations are the following uncoupled system of ordinary differential equations is:

$$\frac{dW}{dx} = \varphi - \frac{1}{kAG}\frac{d}{dx}(EI\frac{d\varphi}{dx}).$$

Finite element formulation

FEM is a numerical method of finding approximate solutions of partial differential equation as well as integral equation. The method essentially consists of assuming the piecewise continuous function for the solution and obtaining the parameters of the functions in a manner that reduces the error in the solution. By this method we divide a beam in to number of small elements and calculate the response for each small elements and finally added all the response to get global value. Stiffness matrix and mass matrix is calculate for each of the discretized element and at last all have to combine to get the global stiffness matrix and mass matrix. The shape function gives the shape of the beam element at anypoint along longitudinal direction. This shape function also calculated by finite element method. Both potential and kinetic energy of beam depends upon the shape function. To obtain stiffness matrix potential energy due to deflection and to obtain mass matrix kinetic energy due to application of sudden load are use. So it can be say that potential and kinetic energy of the beam depends upon shape function of beam obtain by FEM method.

In the present analysis the mathematical formulation and finite element formulation for loaded complex composite beam have been done. The beam is modeled by Timoshenko beam theory. This essentially consists of assuming the piecewise continuous function for the solution and obtaining the parameters of the functions in a manner that reduces the error in the solution.

By this method we divide a beam in to number of small elements and calculate the response for each small elements and finally added all the response to get global value. By taking Timoshenko beam theory we have taken shear deformation into consideration which other theories neglect to make the beam analysis simplified. Due to this we can be able to formulate a composite beam that would be much more reliable for fabrication of structures that are under continuous loading.

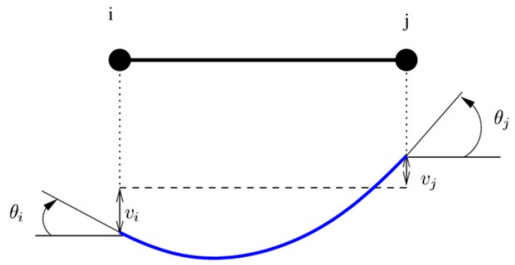

Figure 2.14: Deformation in Timoshenko Beam

Curved geometry

In order to describe initially curved geometry, three configurations: the straight configuration, the stress-free reference configuration, and current configuration, are considered as shown in Fig.(2.15), (2.16). The straight configuration is described by set of parameters or coordinates $X = [X_1 X_2 X_3]^t$, the stress-free curved configuration is defined using the coordinates $X = [X_1 X_2 X_3]^t$, and the current or deformed configuration is described by the vector $r = [r_1 r_2 r_3]^t$. The position vector of an arbitrary point r can be written as $r = X + u$, where$r = [r_1 r_2 r_3]^t$, is the displacement vector. The matrix of position vector gradients J can be written as $J = \frac{\partial r}{\partial X} = \frac{\partial r}{\partial x}\frac{\partial x}{\partial X} = J_e J_0^{-1}$, The matrix J_0 is used to account for the initial stress-free curved geometry. The Green-Lagrange strain tensor $\varepsilon = \frac{1}{2}\left(J^t J - I\right)$, upon using$J = J_e J_0^{-1}$, can be written as $\varepsilon = \frac{1}{2}(J_0^{-1})^t \left(J_e^t J_e J_0^{-1} - I\right)$, which leads to zero strain in the initial stress-free curved configuration.

Geometry representation

The main goal of using the reduced-order model considered in this investigation is to have an accurate representation of the geometry in the reference configuration. elements are related to splines and using linear mapping. Therefore, the mechanics-based elements can be

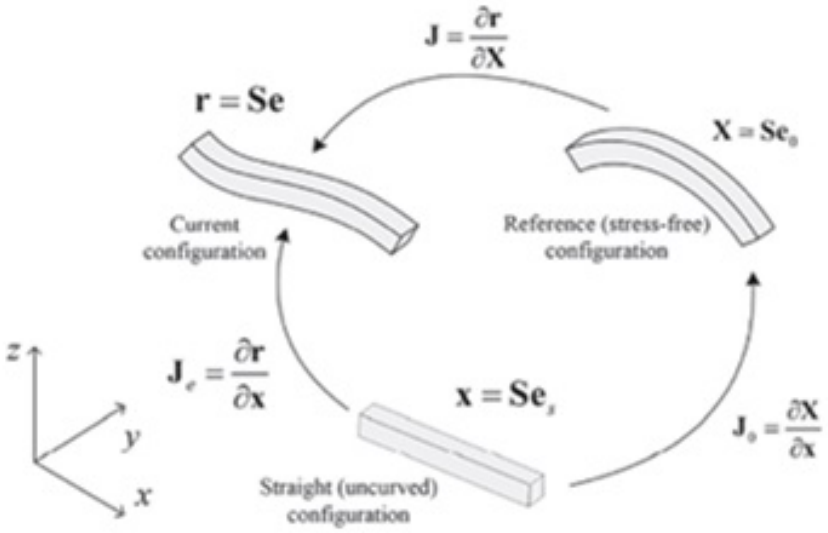

Figure 2.15: Curved geometry

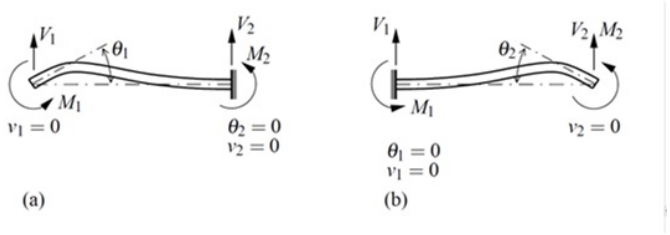

Figure 2.16: Deformation state associated with the activation of θ_1 and θ_2

used as the basis for developing the geometry of the solid models. Using the geometric coefficients, the geometry in the reference configuration is preserved, thereby avoiding any geometry distortion when the analysis is performed. Using the position gradients and the geometric coefficients, no distinction is made between straight and curved elements. By contrast, conventional infinitesimal-rotation elements cannot be related by linear mapping and their use can lead to geometry distortion when the solid models are converted to analysis meshes. This is evident by the high cost and significant time and efforts spent by the industry on converting solid models to analysis meshes. For example, when conventional beam elements are used, multiple straight elements must be used to approximate the curved structures. Other simple examples that demonstrate the geometric representation difficulties encountered when using conventional elements are tapered structures. For these structures, the element thickness varies along the beam axis. The tapering can be easily captured using the element by changing the norms of the transverse gradient vectors at the element nodes as shown in Fig. (2.13), (2.17),(2.18),

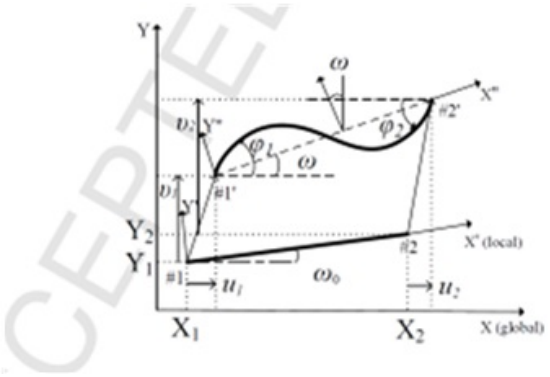

Figure 2.17: Rotationel geometrically nonlinear beam

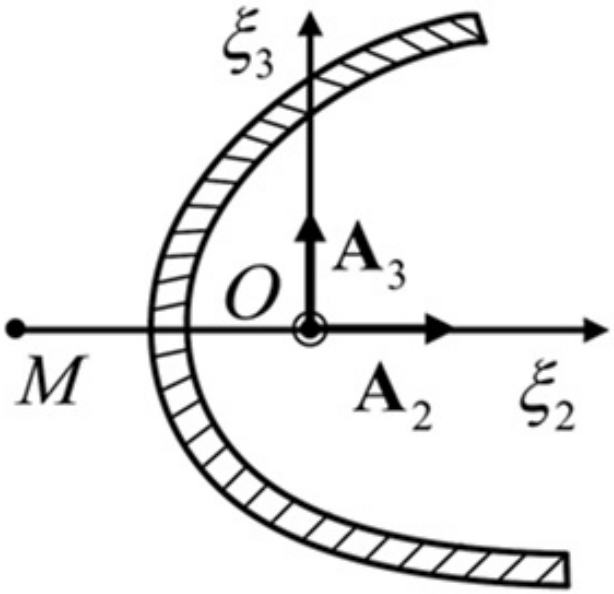

Figure 2.18: Deformation of the beam

(2.19),(2.20), (2.21),(2.22), (2.24),(2).

2.2.1 Conclusion

From preceding illustrative examples results and their discussions, the following can be easily concluded:

• Shows that the effect of shear deformation is to increase the deflection.

• The contribution due to shear deformation to the deflection depends on the modulus ratio $\frac{E}{G}$ as well as the ratio of thickness to length $\frac{t}{L}$.

• The effect of shear deformation is negligible for thin and long beams whereas it is more

Figure 2.19: Deformation of the beam

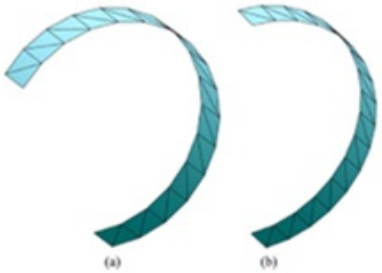

Figure 2.20: Deformation of the beam

significant for beams with thickness-to-length rations $> 1/10$.

• The bending rotation as well as bending moment and axial bending stresses are independent of shear deformation for all statically determinate and indeterminate beams if they obey symmetric boundary condition and loading, whereas for general statically indeterminate beams they will be affected by shear stiffness.

• The described total rotation by Timoshenko is evidentiary apparent and interpreted.

• The superiority of results due mixed formulation is evident in all field variables of the beam problem.

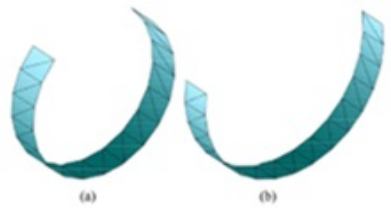

Figure 2.21: Deformation of the beam

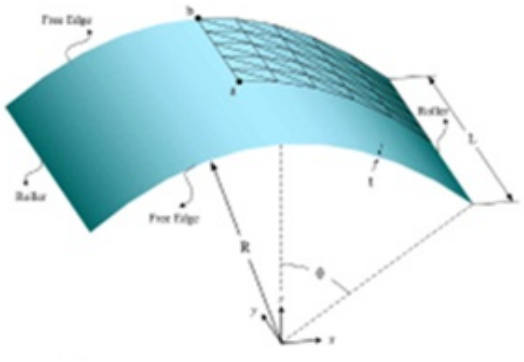

Figure 2.22: Deformation of the beam

Figure 2.23: Deformation of the beam

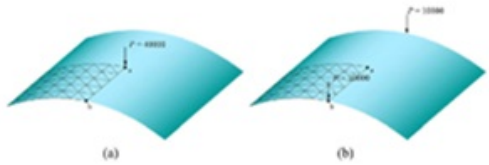

Figure 2.24: Deformation of the beam

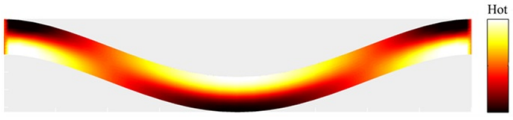

Figure 2.25: Deformation of the beam

Chapter 3

Exponential decay and numerical solution of nonlinear Bresse-Timoshenko system with second sound.

3.1 Introduction and position of the problem:

In the present chapter, we consider the following one dimensional nonlinear Bresse-Timoshenko system with second sound

$$\begin{cases} \rho_1\varphi_{tt} - k\left(\varphi_x + \psi\right)_x + \mu_1\varphi_t = 0 & \text{in} \quad (0,1)\times(0,\infty), \\ -\rho_2\varphi_{ttx} - b\psi_{xx} + k\left(\varphi_x + \psi\right) + \gamma\theta_x + \mathrm{f}\left(\psi\right) = 0 & \text{in} \quad (0,1)\times(0,\infty), \\ \rho_3\theta_t + kq_x + \gamma\psi_{tx} + \lambda\theta = 0 & \text{in} \quad (0,1)\times(0,\infty), \\ \tau_0 q_t + \delta q + k\theta_x = 0 & \text{in} \quad (0,1)\times(0,\infty). \end{cases} \tag{3.1}$$

With the initial and boundary conditions

$$\begin{cases} \varphi(x,0) = \varphi_0(x), \varphi_t(x,0) = \varphi_1(x), \psi(x,0) = \psi_0(x) & \text{in} \quad (0,1), \\ \psi_t(x,0) = \psi_1(x), \theta(x,0) = \theta_0(x), q(x,0) = q_0(x) & \text{in} \quad (0,1), \\ \varphi(0,t) = \varphi(1,t) = \psi(0,t) = \psi(1,t) = q(0,t) & \\ = q(1,t) = \theta(0,t) = \theta\left(1,t\right) = 0 & \text{in} \quad (0,\infty), \end{cases} \tag{3.2}$$

where $t \in (0,+\infty)$ denotes the time variable and $x \in (0,1)$ is the space variable along with the beam of length L, in its equilibrium configuration. Here φ, ψ, θ, q and f(ψ) are specific func-

tions represent, respectively, the transverse displacement of the beam, the rotation angle, the different temperature, the heat flux and forcing term. The coefficients ρ_1, ρ_2, ρ_3, μ_1, τ_0, δ, γ, b, k and λ are positive constants represent the constitutive parameters defining the coupling among the defferent conponents of the materials.

From physical point of view, it is well known that the model using the classic Fourier's law leads to the physical paradox of infinite speed of heat propagation. Many theories have subsequently emerged, to overcome this physical paradox but still keeping the essentials of a heat conduction process. One of which is the advent of the second sound effects observed experimentally in materials at a very low temperature. Second sound effects arise when heat is transported by a wave propagation process instead of the usual diffusion. This theory suggests replacing the classic Fourier's law $\gamma\theta_x + q$, where γ is the coefficient of thermal conductivity and q is the heat flux by a modified law of heat conduction called Cattaneo's law $\gamma\theta_x + q + \tau q_t$. Here, the parameter $\tau > 0$ represents the relaxation time describing the time lag in the response of the heat flux to a gradient in the temperature. The obtained heat system is of hyperbolic type and hence, automatically, eliminating the paradox of infinite speeds. Among the works that have been realised in this fiéeld, we refer the reader to [34, 35]. In the following Figure we introduce the displacements and the rotation angle in the (x_1, x_3) plane as well as the temperature distribution with its contribution to the deformation of the beam as showing in many works for instance [10] where

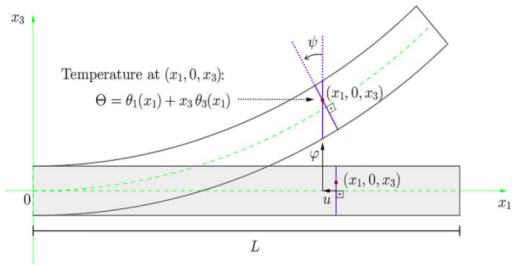

Displacements, rotation angle and temperature distribution in the (x_1, x_3)-plane

- $u = u(x_1, t)$: the longitudinal displacement of points lying on the x_1-axis,
- $\psi = \psi(x_1, t)$: the angle of rotation for the normal to the x_1-axis,

Θ is the Taylor's expansion for the temperature distribution in the (x_1, x_3)-plane (with $x_2 = 0$):

$$\Theta(x_1, x_3, t) = \Theta(x_1, 0, x_3, t) = \theta_1(x, t) + x_3\theta_3(x, t)$$

where θ_1 and θ_3 are temperature components (functions) that may represent the temperature deviations from the reference temperature Θ_0 along the longitudinal and vertical directions.

Elishakoff et al. [27, 28], gave a brief description on the beam model in one-dimensional for beam vibrations. The classical Bernoulli-Euler differential equation ignores rotational inertia and shear deformation. It is given by

$$EI\varphi_{xxxx} + \rho A\varphi_{tt} = 0, \tag{3.3}$$

where E is the modulus of elasticity, I is the moment of inertia, $\varphi(x,t)$ is the transverse displacement, x is the axial coordinate, t is the time, ρ is the material density, and A is the cross-sectional area.

Later, Bresse [19] and Rayleigh extended and corrected the Bernoulli-Euler equation (3.3), by taking into account the rotary movement of the beam elements. The angle of rotation equals the slope of the deflection curve φ_x, the associated angular acceleration is φ_{xtt}. As a result, the moment of inertia of the element about an axis through its center of mass equals $\rho I\varphi_{xtt}dx$ and according to D'Alembert's principle, we obtain

$$-V + M_x - \rho I\varphi_{xtt} = 0, \tag{3.4}$$

where $V(x,t)$ is the shearing force and $M(x,t)$ the bending moment.

Replacing this equation in the case of dynamic equilibrium with the forces of transverse vibration, we have

$$V_x = -\rho A\varphi_{tt} = (M_x - \rho I\varphi_{xtt})_x. \tag{3.5}$$

Physically from elastic theory, we have $M = EI\varphi_{xx}$, then it results in a Rayleigh model for the uniform beam oscillations given by

$$EI\varphi_{xxxx} + \rho A\varphi_{tt} - \rho I\varphi_{xxtt} = 0, \tag{3.6}$$

we call equation (3.6) the rotatory inertial.

Afterwards, Timoshenko [48] extended the equation (3.6) by adding the impact of the shear deformation, expressing the slope of the deflection curve in two parts

$$\varphi_x = -\psi + \zeta, \tag{3.7}$$

ψ as the rotation of the cross-sections with the neglection of the shear deformation and ζ as the angle associated with the shear deformation at the neutral axis in the same cross-section.

On the other hand, according to the mechanics of solid we can write

$$M = EI\psi_x, \tag{3.8}$$

$$V = k_1\zeta AG = k_1 AG(\varphi_x + \psi), \tag{3.9}$$

where k_1 is the shear coefficient and G is the shear modulus.

The state of dynamic equilibrium of forces in the vertical direction is given by

$$\rho A\varphi_{tt} - V_x = 0. \tag{3.10}$$

Deriving with respect to the in equation (3.7) and by substituting in the dynamic equilibrium equation of motion (3.4), we get

$$-V + M_x + \rho I\psi_{tt} = 0. \tag{3.11}$$

The Timoshenko system, was obtained by substituting respectively (3.9) and (3.8) into (3.10) and (3.11), thus

$$-k_1 AG(\varphi_x + \psi)_x + \rho A\varphi_{tt} = 0. \tag{3.12}$$

$$-k_1 AG(\varphi_x + \psi) + EI\psi_{xx} + \rho I\psi_{tt} = 0, \tag{3.13}$$

where,

$\rho_1 = \rho A$ is the mass density,

$\rho_2 = \rho I$ is the moment mass inertia,

$b = EI$ is the rigidity coefficient (of the cross-section),

$k = k_1 AG$ is the shear modulus of elasticity.

Then, the Timoshenko system takes the following form

$$\begin{cases} \rho_1\varphi_{tt} - k\left(\varphi_x + \psi\right)_x = 0, \\ \rho_2\psi_{tt} - b\psi_{xx} + k\left(\varphi_x + \psi\right) = 0. \end{cases} \tag{3.14}$$

It should be noticed that mentioned problem plays a crucial role in engineering applications. And for more details on the valuable resources that have been realised regarding Timoshenko system, we refer the readers to [5, 11, 12, 13, 14, 15, 16, 30, 33, 38, 39, 48, 52].

Elishakoff [26], by differentiating the Timoshenko hypotheses (3.7) with respect to t, we get

$$\psi_{tt} = -\varphi_{ttx}. \tag{3.15}$$

Inserting (3.15) in $(3.14)_2$, we obtain the well-known Bresse-Timoshenko system by combining d'Alembert's concept for dynamic equilibrium, with Timoshenko hypothesis to get the following system

$$\begin{cases} \rho_1\varphi_{tt} - k\left(\varphi_x + \psi\right)_x = 0, \\ -\rho_2\varphi_{ttx} - b\psi_{xx} + k\left(\varphi_x + \psi\right) = 0. \end{cases} \tag{3.16}$$

For more details, we refer [8, 9, 22, 26, 29].

Many investigations have been realised concerning the asymptotic behavior of the solution of Bresse-Timoshenko system. Among them, we cite the work of Almeida and Ramos [6], who they considered the following system

$$\begin{cases} \rho_1\varphi_{tt} - \beta\left(\varphi_x + \psi\right)_x = 0, \\ -\rho_2\varphi_{ttx} - b\psi_{xx} + \beta\left(\varphi_x + \psi\right) + \mu_1\psi_t = 0, \end{cases} \tag{3.17}$$

where they showed that the viscous damping acting on angle rotation of the above system is strong enough to provoke an exponential decay of the solution. Junior et al. [7] considered the following system

$$\begin{cases} \rho_1\varphi_{tt} - \beta\left(\varphi_x + \psi\right)_x + \mu_1\psi_t = 0, \\ -\rho_2\varphi_{ttx} - b\psi_{xx} + \beta\left(\varphi_x + \psi\right) = 0, \end{cases} \tag{3.18}$$

and they showed that the mechanism damping given by the viscous damping acting on the transverse displacement of the beam stabilizes exponantially the system.

Kh. Zennir et al. [51] studied the following nonlinear Bresse-Timoshenko system

$$\begin{cases} \rho_1\partial_{tt}\varphi - k\left(\varphi_x + \psi\right)_x + \sigma_1\partial_t\varphi = 0, \\ -\rho_2\partial_{tt}\varphi_x - \alpha\psi_{xx} + k\left(\varphi_x + \psi\right) - \xi_1\theta_x \\ \qquad -\xi_2 p_x + \sigma_2\mathcal{G}(\partial_t\psi) = 0, \\ c\partial_t\theta + d\partial_t p - k\theta_{xx} - \xi_1\partial_t\psi_x = 0, \\ d\partial_t\theta + r\partial_t p - hp_{xx} - \xi_2\partial_t\psi_x = 0. \end{cases} \tag{3.19}$$

The authors proved the well-posedness of the system by using the classical Faedo-Galerkin approximations and showed a general decay result of the system.

Motivated by the previous works, in this thesis we give a global existence and regularity results, which can be proved by using the standard Feado-Galerkin method. Moreover, we show that the dissipation given by the second sound is strong enough to give an exponential stabilityof solution of the system (3.40) by using the energy method, that requires to constract an appropriate Lyapunov functional which allows us to estimate the energy of the system (3.40) and to show that it decays an exponetial manner without any conditions on the coefficients of the system. Importance of this complimantary control and his influence on the asymptotic behavior of the solution appears in many works for the different types of problems such as [11, 31, 33]. Finally, some of the numerical simulation results are obtained using MATLAB software.

The rest of this thesis is organized as follows: In Section 2, we recall some preliminaries, we state without proof a global existence and regularity result of the problem (3.40). In Section 3, we estabilish the exponential stability result. In Section 4, we validate our theoretical stability result by numerical approximation.

3.2 Preliminaries and main results

In this section, we present and recall some mathematical notions to be used for the proof of the stability result.

$(\mathcal{A})$ $\mathrm{f}:\mathbb{R}\to\mathbb{R}$ satisfies

$$|\mathrm{f}(\psi^2)-\mathrm{f}(\psi^1)|\leq k_0(|\psi^1|^{\varrho}+|\psi^2|^{\varrho})|\psi^1-\psi^2| \quad \text{and} \quad \psi^1\in\mathbb{R},\psi^2\in\mathbb{R}, \tag{3.20}$$

where $k_0>0$, $\varrho>0$. In addition, we assume that

$$0\leq\widehat{\mathrm{f}}(\psi)\leq\psi\mathrm{f}(\psi) \quad \text{implies} \quad -\psi\mathrm{f}(\psi)\leq-\widehat{\mathrm{f}}(\psi)\leq 0,\psi\in\mathbb{R}, \tag{3.21}$$

with

$$\widehat{\mathrm{f}}(\psi)=\int_0^{\psi}\mathrm{f}(s)ds. \tag{3.22}$$

Here are the functional inequalities that helps us leter in some estimations to achieve our stability result, we recall in the following Young's inequality [20] given by

$$ab\leq\frac{|a|^p}{p}+\frac{|b|^q}{q}, \quad \forall a,b\in\mathbb{R}, \quad \left(\frac{1}{p}+\frac{1}{q}=1,p>1,q>1\right).$$

According to Young's inequality, for all $\varepsilon > 0$, and $p = q = 2$ we obtain

$$ab \leq \varepsilon a^2 + \frac{1}{4\varepsilon} b^2. \tag{3.23}$$

Together with Poincare's inequality [20] given by

$$\int_I u^2 dx \leq C \int_I u_x^2 dx, \quad \forall u \in H_0^1(I), \tag{3.24}$$

where I is a bounded interval and C is a constant (depending on $|I| < \infty$).

Remark 3.2.1. We have

$$-2(\varphi_x + \psi)\psi \leq (\varphi_x + \psi)^2 + \psi^2,$$

and, on the other hand, we also have

$$(\varphi_x + \psi - \psi)^2 = (\varphi_x + \psi)^2 + \psi^2 - 2(\varphi_x + \psi)\psi \leq 2(\varphi_x + \psi)^2 + 2\psi^2.$$

Finally, by integreting and using Poincaré inequality (3.24), we obtain the following inequality

$$\int_0^1 \varphi_x^2 dx \leq 2 \int_0^1 (\varphi_x + \psi)^2 dx + 2 \int_0^1 \psi_x^2 dx, \tag{3.25}$$

where $C = \frac{1}{|I|} \geq 0$.

3.3 Well- posedness of the problem

For completeness, we state without proof the following global existence and regularity result which can be proved by using the standard Feado-Galerkin method, for this we refer the reader to [4, 47, 51].

Theorem 3.3.1. *Let* $(\varphi_0, \varphi_1) \in H_0^1(0,1) \times L^2(0,1), (\psi_0, \psi_1) \in H_0^1(0,1) \times L^2(0,1)$ *and* $(\theta_0, q_0) \in L^2(0,1) \times L^2(0,1)$ *be given. Assume that* $(\mathcal{A})$ *are satisfied, then the problem* (3.40)-(3.27) *has a unique global (weak) solution satisfying*

$$\varphi, \psi \in \mathcal{C}(\mathbb{R}_+, H_0^1(0,1)) \cap \mathcal{C}^1(\mathbb{R}_+, L^2(0,1)),$$

$$\theta, q \in \mathcal{C}(\mathbb{R}_+, L^2(0,1)).$$

.

Proof. By Using Faedo-Galerkin approximations, we prove the existence of unique global solution of (1.2)- (1.4). For more detail, we refer the reader to see [4, 12, 14].

Step one: Approximate the problem

Let $\{u_j\}$, $\{v_j\}, \{\theta_j\}, \{P_j\}$ be the Galerkin basis, For $n \geq 1$, let

$$W_n = span\{u_1, u_2, ..., u_n\}$$

$$K_n = span\{v_1, v_2, ..., v_n\}$$

$$\Theta_n = span\{\theta_1, \theta_2, ..., \theta_n\}$$

$$\Gamma_n = span\{P_1, P_2, ..., P_n\},$$

given initial data $(\varphi_0, \psi_0) \in H_0^1(0,1) \times H_0^1(0,1), \varphi_1, \varphi_2, \varphi_3 \in L^2(0,1)$ and $\theta_0, P_0 \in L^2(0,1)$ we define the approximations

$$\varphi_n = \sum_{j=1}^{n} g_{jn}(t) u_j(x)$$

$$\psi_n = \sum_{j=1}^{n} \zeta_{jn}(t) v_j(x)$$

$$\theta_n = \sum_{j=1}^{n} f_{jn}(t) \theta_j(x)$$

$$P_n = \sum_{j=1}^{n} k_{jn}(t) P_j(x),$$

which satisfy the following approximate problem

$$\begin{cases} \rho_1 (\varphi_{ttn}, u_j) - k ((\varphi_{xn} + \psi_n), u_{jx}) + \mu_1 (\varphi_{tn}, u_j) = 0 & \text{in} \quad (0,1) \times (0,\infty), \\ -\rho_2 (\varphi_{ttxn}, u_{jx}) - b (\psi_{xxn}, v_{jx}) + k ((\varphi_{xn} + \psi_n), u_j) + \gamma (\theta_{xn}, \theta_j) + (\mathrm{f}(\psi_n), v_j) = 0 & \text{in} \quad (0,1) \times (0,\infty), \\ \rho_3 (\theta_{tn}, \theta_j) + k (q_{xn}, P_j) + \gamma (\psi_{txn}, v_j) + \lambda (\theta_n, \theta_j) = 0 & \text{in} \quad (0,1) \times (0,\infty), \\ \tau_0 (q_{tn}, P_j) + \delta (q_n, P_j) + k (\theta_{xn}, \theta_{xj}) = 0 & \text{in} \quad (0,1) \times (0,\infty), \end{cases} \tag{3.26}$$

with initial conditions

$$\begin{cases} \varphi_n(x,0) = \varphi_0^n(x), \varphi_{tn}(x,0) = \varphi_1^n(x), \psi_n(x,0) = \psi_0^n(x) & \text{in} \quad (0,1), \\ \psi_{tn}(x,0) = \psi_1^n(x), \theta_n(x,0) = \theta_0^n(x), q_n(x,0) = q_0^n(x) & \text{in} \quad (0,1), \\ \varphi_n(0,t) = \varphi_n(1,t) = \psi_n(0,t) = \psi_n(1,t) = q_n(0,t) & \\ = q_n(1,t) = \theta_n(0,t) = \theta_n(1,t) = 0 & \text{in} \quad (0,\infty), \end{cases} \tag{3.27}$$

which satisfies

$$\varphi_0^n \to \varphi_0, \text{strongly in } H_0^1(0,1)$$

$$\varphi_1^n \to \varphi_1, \text{strongly in } L^2(0,1)$$

$$\varphi_2^n \to \varphi_2, \text{strongly in } L^2(0,1)$$

$$\varphi_3^n \to \varphi_3, \text{strongly in } L^2(0,1)$$

$$\psi_0^n \to \psi_0, \text{strongly in } H_0^1(0,1)$$

$$\psi_1^n \to \psi_1, \text{strongly in } L^2(0,1)$$

$$\theta_0^n \to \theta_0, \text{strongly in } L^2(0,1)$$

$$P_0^n \to P_0, \text{strongly in } L^2(0,1).$$

By using the Caratheodory Theorem for standard ordinary differential equations theory, the problem (3.2) and (3.3) has a solutions $(g_{jn}(t), \zeta_{jn}(t), f_{jn}(t), k_{jn}(t))_{j=1\ldots n} \in (H^3(0,1))^4$ and by using the embedding $H^m(0,1) \to C^m(0,1)$, we deduce that the solution $(g_{jn}(t), \zeta_{jn}(t), f_{jn}(t), k_{jn}(t))_{j=1\ldots n} \in (C^2(0,1))^4$. In turn, this gives a unique $(\varphi_n, \psi_n, \theta_n, P_n)$ defined by (3.1) and satisfying (3.2).

Second step: The first a priori estimate

Multiplying equations of (3.2) by $\partial_t g_{jn}, \partial_t h_{jn} \partial_t f_{jn}$ and $\partial_t k_{jn}$ respectively and using

$$\begin{aligned} k\int_0^1 \varphi_{tt}\psi_{tx}dx = &\int_0^1 \psi_t\left[-\rho_2\varphi_{ttx}(x,t) - b\psi_{xx}(x,t)\right]dx \\ &+ \int_0^1 \psi_t\left[k(\varphi_x+\psi)(x,t)\right]dx \\ &+ \int_0^1 \psi_t\left[\varphi\theta_x(x,t) + \mathrm{f}(\psi)(x,t)\right]dx = 0, \end{aligned}$$

we get

$$\begin{aligned} &\frac{d}{2dt}\left[\rho_1\int_0^1 \varphi_{nt}^2dx + k\int_0^1(\varphi_{nx}+\psi_n)^2dx + \frac{\rho_1\rho_2}{K}\int_0^1\varphi_{ntt}^2dx\right] \\ &\quad + \frac{d}{2dt}\left[\rho_2\int_0^1\varphi_{ntx}^2dx + b\int_0^1\psi_{nx}^2dx + \rho_3\int_0^1\theta_n^2dx + \tau_0\int_0^1 q_n^2dx + 2\widehat{\mathrm{f}}(\psi_n)\right] \\ &\quad + \mu_1\int_0^1\varphi_{nt}^2dx + \frac{\mu_1\rho_2}{k}\int_0^1\varphi_{ntt}^2dx + \delta\int_0^1 q_n^2dx + \varphi_n\int_0^1\theta_n^2dx = 0. \end{aligned} \tag{3.28}$$

Now integrating (3.5) and by using $(2.3)_1$, we have

$$\mathcal{E}_n(t) + \mu_1\int_0^t\int_0^1\varphi_{nt}^2dx + \frac{\mu_1\rho_2}{k}\int_0^t\int_0^1\varphi_{ntt}^2dx + \delta\int_0^t\int_0^1 q_n^2dx + \varphi_n\int_0^t\int_0^1\theta_n^2dx = 0, \tag{3.29}$$

with

$$\mathcal{E}_n(t) = \frac{1}{2}\int_0^1 \Big[\rho_1\varphi_{nt}^2 + k(\varphi_{nx}+\psi_n)^2 + \frac{\rho_1\rho_2}{k}\varphi_{ntt}^2 + \rho_2\varphi_{ntx}^2 + b\psi_{nx}^2\Big]\,dx + \frac{1}{2}\int_0^1 \Big[\rho_3\theta_n^2 + \tau_0 q_n^2 + 2\widehat{\mathrm{f}}(\psi_n)\Big]\,dx, \tag{3.30}$$

then

$$\mathcal{E}_n(t) \le \mathcal{E}_n(0).$$

Thus, there exists a positive constant C independent on n such that

$$\mathcal{E}_n(t) \le C, \quad t \ge 0.$$

By (2.1) and (3.9), we have

$$\int_0^1 \big[\varphi_{nt}^2 + (\varphi_{nx}+\psi_n)^2 + \varphi_{ntt}^2 + \varphi_{ntx}^2 + b\psi_{nx}^2\big]\,dx + \int_0^1 \Big[\rho_3\theta_n^2 + \tau_0 q_n^2 + 2\widehat{\mathrm{f}}(\psi_n)\Big]\,dx \le C. \tag{3.31}$$

Then $t_n = T$, for all $T > 0$.

Third step: The second a priori estimate Differentiating $(3.2)_1$ and multiplying by $\partial_{tt}\varphi_n$, integrating the result over $(0,1)$, we get

$$\sigma_1\int_0^1 \varphi_{nt}^2 + k\int_0^1 (\varphi_{nxt}+\psi_{nt})\varphi_{nxtt} + \frac{\rho_1}{2}\int_0^1 \varphi_{nttt}^2 = 0, \tag{3.32}$$

differentiating $(3.2)_2$ and multiplying by $\partial_{tt}\psi_n$, using the fact that

$$\psi_{tnx} = \frac{\rho_1}{k}\varphi_{tttn}(x,t) + \frac{\mu_1}{k}\varphi_{ttn}(x,t) - \varphi_{nxxt}(x,t). \tag{3.33}$$

Then integrating the result over $(0,1)$, using $(2.3)_2$, we get

$$\frac{\rho_1\rho_2}{2k}\frac{d}{dt}\int_0^1 \varphi_{ttn}^2 dx + \frac{\rho_2}{2}\frac{d}{dt}\int_0^1 \varphi_{txn}^2 dx + \frac{b}{2}\frac{d}{dt}\int_0^1 \psi_{xn}^2 dx + k\int_0^1 (\varphi_{xn}+\psi_n)\psi_{tn}dx + \frac{\mu_1\rho_2}{k}\int_0^1 \varphi_{ttn}^2 dx + \gamma\int_0^1 \theta_{xn}\psi_{tn}dx + \frac{d}{dt}\int_0^1 \widehat{\mathrm{f}}(\psi_n)dx = 0. \tag{3.34}$$

Differentiating the equations of (3.2), multiplying by $\partial_t\theta_n, \partial_{tt}P_n$ and then integrating the result over $(0,1)$, we get

$$\frac{\rho_3 d}{2dt}\int_0^1 \theta_n^2 dx + k\int_0^1 q_{xn}\theta dx - \gamma\int_0^1 \theta_{xn}\psi_{tn}dx + \lambda\int_0^1 \theta_n^2 dx = 0, \tag{3.35}$$

$$\frac{\tau_0 d}{2dt}\int_0^1 q_n^2 dx - k\int_0^1 q_{nx}\theta dx + \delta\int_0^1 q_n^2 dx = 0. \tag{3.36}$$

Combining (3.11) and (3.12), we get

$$\mathcal{R}_n(t)+\frac{\rho_3 d}{2dt}\int_0^t\int_0^1 \theta_n^2 dx + k\int_0^t\int_0^1 q_{xn}\theta dx - \gamma\int_0^t\int_0^1 \theta_{xn}\psi_{tn}dx + \lambda\int_0^t\int_0^1 \theta_n^2 dx \tag{3.37}$$

$$+\frac{\tau_0 d}{2dt}\int_0^t\int_0^1 q_n^2 dx - k\int_0^t\int_0^1 q_{nx}\theta dx + \delta\int_0^t\int_0^1 q_n^2 dx = \mathcal{R}_n(0). \tag{3.38}$$

Where

$$\mathcal{R}_n(t) = \frac{1}{2}\int_0^1 \left[\rho_1\varphi_{nt}^2 + k(\varphi_{nx}+\psi_n)^2 + \frac{\rho_1\rho_2}{k}\varphi_{ntt}^2 + \rho_2\varphi_{ntx}^2 + b\psi_{nx}^2\right]dx$$

$$+\frac{1}{2}\int_0^1 \left[\rho_3\theta_n^2 + \tau_0 q_n^2 + 2\widehat{\mathrm{f}}(\psi_n)\right]dx, \tag{3.39}$$

as in the fist a priori estimate, there exists $C>0$ independent on n such that

$$\mathcal{R}_n(t)\leq C, \quad t\geq 0.$$

Fourth step: Passage to limit

From (3.10) and (3.14), we conclude that for any $n\in\mathbb{N}$,

$$\varphi_n \quad \text{is bounded in } L^\infty(\mathbb{R}_+, H_0^1(0,1))$$

$$\partial_t\varphi_n \quad \text{is bounded in } L^\infty(\mathbb{R}_+, L^2(0,1))$$

$$\partial_{tt}\varphi_n \quad \text{is bounded in } L^\infty(\mathbb{R}_+, L^2(0,1))$$

$$\psi_n \quad \text{is bounded in } L^\infty(\mathbb{R}_+, H_0^1(0,1))$$

$$\partial_t\psi_n \quad \text{is bounded in } L^\infty(\mathbb{R}_+, L^2(0,1))$$

$$\theta_n \quad \text{is bounded in } L^\infty(\mathbb{R}_+, L^2(0,1))$$

$$\partial_t\theta_n \quad \text{is bounded in } L^\infty(\mathbb{R}_+, L^2(0,1))$$

$$P_n \quad \text{is bounded in } L^\infty(\mathbb{R}_+, L^2(0,1))$$

$$\partial_t P_n \quad \text{is bounded in } L^\infty(\mathbb{R}_+, L^2(0,1)).$$

Thus we get

$$\varphi_n \quad \text{weakly star in } L^2(\mathbb{R}_+, H_0^1(0,1))$$

$$\partial_t\varphi_n \quad \text{weakly star in } L^2(\mathbb{R}_+, L^2(0,1))$$

$$\partial_{tt}\varphi_n \quad \text{weakly star in } L^2(\mathbb{R}_+, L^2(0,1))$$

$$\psi_n \quad \text{weakly star in } L^2(\mathbb{R}_+, H_0^1(0,1))$$

$$\partial_t\psi_n \quad \text{weakly star in } L^2(\mathbb{R}_+, L^2(0,1))$$

$$\theta_n \quad \text{weakly star in } L^2(\mathbb{R}_+, L^2(0,1))$$

$$\partial_t\theta_n \quad \text{weakly star in } L^2(\mathbb{R}_+, L^2(0,1))$$

$$P_n \quad \text{weakly star in } L^2(\mathbb{R}_+, L^2(0,1))$$

$$\partial_t P_n \quad \text{weakly star in } L^2(\mathbb{R}_+, L^2(0,1)).$$

By (3.17), we deduce that φ_n, ψ_n is bounded in $L^2(\mathbb{R}_+, H_0^1(0,1)$ and $\partial_t\varphi_n, \partial_{tt}\varphi_n$ are bounded in $L^2(\mathbb{R}_+, L^2(0,1)$, and $\partial_t\theta_n, \partial_t P_n$ are bounded in $L^2(\mathbb{R}_+, L^2(0,1)$. Then from Aubin-Lions theorem [18], we infer that for and, $T > 0$,

$$\varphi_n \quad \text{strongly in } L^\infty(\mathbb{R}_+, H_0^1(0,1))$$

$$\psi_n \quad \text{strongly in } L^\infty(\mathbb{R}_+, H_0^1(0,1))$$

$$\theta_n \quad \text{strongly in } C^0(\mathbb{R}_+, L^2(0,1))$$

$$P_n \quad \text{strongly in } L^\infty(\mathbb{R}_+, L^2(0,1)).$$

We also obtain by Lemma 1.4 in Kim [15] that

$$\varphi_n \quad \text{strongly in } C(0,T, H_0^1(0,1))$$

$$\psi_n \quad \text{strongly in } C(0,T, H_0^1(0,1))$$

$$\theta_n \quad \text{strongly in } C(0,T, L^2(0,1))$$

$$P_n \quad \text{strongly in } C(0,T, L^2(0,1)).$$

Then we can pass to limit the approximate problem (3.2) and (3.3) in order to get a weak solution of problem (1.2)-(1.4).

Step Six: Continuous dependence and uniqueness We prove the continuous dependence of unique solution of (1.2)-(1.4).

Let $(\varphi, \varphi_t, \varphi_{tt}, \psi, \Upsilon, \Psi)$ and $(\Gamma, \Gamma_t, \Gamma_{tt}, \Xi, \Pi, \Omega)$ be two global solutions of (1.2)?(1.4) with respect to initial data $(\varphi_0, \varphi_1, \varphi_2, \psi_0, \Theta, \Psi)$ and $(\Gamma_0, \Gamma_1, \Gamma_2, \Xi_0, \Phi_0, \Omega_0)$. Let

$$\Lambda(t) = \varphi - \Gamma$$

$$\Sigma(t) = \psi - \Xi$$

$$\chi(t) = \Pi - \Phi$$

$$M(t) = \Psi - \Omega.$$

Then $(\Lambda, \Sigma, \chi, M)$ verifies (1.2)-(1.4) and we have

$$\begin{cases} \rho_1 \Lambda_{tt} - k\left(\Lambda_x + \Sigma\right)_x + \mu_1 \Lambda_t = 0 & \text{in} \quad (0,1)\times(0,\infty), \\ -\rho_2 \Lambda_{ttx} - b\Sigma_{xx} + k\left(\Lambda_x + \Sigma\right) + \gamma\chi_x + \mathrm{f}\left(\Sigma\right) = 0 & \text{in} \quad (0,1)\times(0,\infty), \\ \rho_3 \chi_t + kM_x + \gamma\Sigma_{tx} + \lambda\chi = 0 & \text{in} \quad (0,1)\times(0,\infty), \\ \tau_0 M_t + \delta M + k\chi_x = 0 & \text{in} \quad (0,1)\times(0,\infty). \end{cases} \tag{3.40}$$

Multiplying $(3.21)_1$ by Λ_t, $(3.21)_2$ by Σ_t integrating over $(0,1)$ and since

$$\begin{aligned} k\int_0^1 \Lambda_{tt}\Sigma_{tx}dx = &\int_0^1 \Sigma_t\left[-\rho_2\Lambda_{ttx}(x,t) - b\Sigma_{xx}(x,t)\right]dx \\ &+ \int_0^1 \Sigma_t\left[k(\Lambda_x+\Sigma)(x,t)\right]dx \\ &+ \int_0^1 \Sigma_t\left[\gamma\theta_x(x,t) + \mathrm{f}(\Sigma)(x,t)\right]dx = 0, \end{aligned}$$

we get

$$\begin{aligned} &\frac{d}{2dt}\left[\rho_1\int_0^1 \Lambda_t^2 dx + k\int_0^1 (\Lambda_x+\Sigma)^2 dx + \frac{\rho_1\rho_2}{K}\int_0^1 \Lambda_{tt}^2 dx\right] \\ &\quad + \frac{d}{2dt}\left[\rho_2\int_0^1 \Lambda_{tx}^2 dx + b\int_0^1 \Sigma_x^2 dx + \rho_3\int_0^1 \chi^2 dx + \tau_0\int_0^1 q^2 dx + 2\widehat{\mathrm{f}}(\Sigma)\right] \\ &\quad + \mu_1\int_0^1 \Lambda_t^2 dx + \frac{\mu_1\rho_2}{k}\int_0^1 \Lambda_{tt}^2 dx + \delta\int_0^1 M^2 dx + \lambda\int_0^1 \chi^2 dx = 0. \end{aligned} \tag{3.41}$$

Then

$$\mathcal{E}'(t) \leq 0 \tag{3.42}$$

$$\begin{aligned} \mathcal{E}'(t) \leq & C[\int_0^1 \Lambda_t^2 dx + \int_0^1 \Lambda_{tx}^2 dx + \int_0^1 (\Lambda_x+\Sigma)^2 dx \\ &+ \int_0^1 \Lambda_{tt}^2 dx + \int_0^1 \Sigma_x^2 dx + \int_0^1 \chi^2 dx \\ &+ \int_0^1 M^2 dx + \int_0^1 \widehat{\mathrm{f}}(\Sigma)dx], \end{aligned} \tag{3.43}$$

where

$$\mathcal{E}(t)=\frac{1}{2}\int_0^1\Big[\rho_1\Lambda_t^2+k(\Lambda_x+\Sigma)^2+\frac{\rho_1\rho_2}{k}\Lambda_{tt}^2+\rho_2\Lambda_{tx}^2+b\Sigma_x^2\Big]\,dx + \frac{1}{2}\int_0^1\Big[\rho_3\chi^2+\tau_0M^2+2\widehat{\mathrm{f}}(\Sigma)\Big]\,dx, \tag{3.44}$$

by integrating (3.23), we get

$$\mathcal{E}(t)\le\mathcal{E}(0)+C_1\int_0^1\left[\|\Lambda_t^2\|+\|(\Lambda_x+\Sigma)^2\|+\|\Lambda_{tt}^2\|+\|\Lambda_{tx}^2\|+\|\Sigma_x^2\|\right]dx + C_1\int_0^1\left[\|\chi^2\|+\|M^2\|\right]dx. \tag{3.45}$$

On the other hand, we have

$$\mathcal{E}(t)\ge C_0\left[\|\Lambda_t^2\|+\|(\Lambda_x+\Sigma)^2\|+\|\Lambda_{tt}^2\|+\|\Lambda_{tx}^2\|+\|\Sigma_x^2\|\right]dx + C_0\left[\|\chi^2\|+\|M^2\|\right]dx, \tag{3.46}$$

owing to Gronwall's inequality to (3.27), we have

$$\left[\|\Lambda_t^2\|+\|(\Lambda_x+\Sigma)^2\|+\|\Lambda_{tt}^2\|+\|\Lambda_{tx}^2\|+\|\Sigma_x^2\|\right]dx + \left[\|\chi^2\|+\|M^2\|\right]dx\le e^{c_2t}\mathcal{E}(0), \tag{3.47}$$

which implies that solution of (1.2)?(1.4) depends continuously on the initial data. □

3.4 Exponential stability

In this section, we use the energy method to establish the exponential stability of the system (3.40)-(3.27). To achieve our goal, we state and prove the following lemmas.

Lemma 3.4.1. *Let (φ,ψ,θ,q) be a solution of (3.40)-(3.27). Then, the energy functional $\mathcal{E}(t)$, defined by*

$$\mathcal{E}(t)=\frac{1}{2}\int_0^1\Big[\rho_1\varphi_t^2+k(\varphi_x+\psi)^2+\frac{\rho_1\rho_2}{k}\varphi_{tt}^2+\rho_2\varphi_{tx}^2+b\psi_x^2\Big]\,dx + \frac{1}{2}\int_0^1\Big[\rho_3\theta^2+\tau_0q^2+2\widehat{\mathrm{f}}(\psi)\Big]\,dx, \tag{3.48}$$

satisfies

$$\mathcal{E}'(t)=-\mu_1\int_0^1\varphi_t^2dx-\frac{\mu_1\rho_2}{k}\int_0^1\varphi_{tt}^2dx-\delta\int_0^1q^2dx-\lambda\int_0^1\theta^2dx\le0 \tag{3.49}$$

Proof. Multiplying $(3.40)_1$, $(3.40)_2$, $(3.40)_3$ and $(3.40)_4$, by φ_t, ψ_t, θ and q respectively, and an integration by parts over $(0,1)$, we get

$$\begin{cases} \int_0^1 \varphi_t \left[\rho_1\varphi_{tt}(x,t) - k(\varphi_x+\psi)_x(x,t)\right] \\ \qquad + \int_0^1 \varphi_t \left[\mu_1\varphi_t(x,t)\right] dx = 0 & \text{in} \quad (0,1)\times(0,\infty), \\ \int_0^1 \psi_t \left[-\rho_2\varphi_{ttx}(x,t) - b\psi_{xx}(x,t)\right] dx \\ \qquad + \int_0^1 \psi_t \left[k(\varphi_x+\psi)(x,t)\right] dx \\ \qquad + \int_0^1 \psi_t \left[\gamma\theta_x(x,t) + \mathrm{f}(\psi)(x,t)\right] dx = 0 & \text{in} \quad (0,1)\times(0,\infty), \\ \int_0^1 \theta \left[\rho_3\theta_t(x,t) + kq_x(x,t) + \gamma\psi_{tx}(x,t)\right] dx \\ \qquad + \int_0^1 \theta \left[\lambda\theta(x,t)\right] dx = 0 & \text{in} \quad (0,1)\times(0,\infty), \\ \int_0^1 q \left[\tau_0 q_t(x,t) + \delta q\,(x,t) + k\theta_x(x,t)\right] dx = 0 & \text{in} \quad (0,1)\times(0,\infty). \end{cases} \tag{3.50}$$

Using integration by parts in (3.50) and the boundary conditions (3.27), yield

$$(3.50)_1 \Leftrightarrow \frac{\rho_1 d}{2dt}\int_0^1 \varphi_t^2 dx + k\int_0^1 (\varphi_x+\psi)\varphi_{tx}dx + \mu_1\int_0^1 \varphi_t^2 dx = 0, \tag{3.51}$$

$$\begin{aligned}(3.50)_2 \Leftrightarrow \frac{bd}{2dt}\int_0^1 \psi_x^2 dx + k\int_0^1 (\varphi_x+\psi)\psi_t dx + \rho_2\int_0^1 \varphi_{tt}\psi_{tx}dx \\ + \gamma\int_0^1 \theta_x\psi_t dx + \frac{d}{dt}\int_0^1 \widehat{\mathrm{f}}(\psi)dx = 0,\end{aligned} \tag{3.52}$$

$$(3.50)_3 \Leftrightarrow \frac{\rho_3 d}{2dt}\int_0^1 \theta^2 dx + k\int_0^1 q_x\theta dx - \gamma\int_0^1 \theta_x\psi_t dx + \lambda\int_0^1 \theta^2 dx = 0, \tag{3.53}$$

$$(3.50)_4 \Leftrightarrow \frac{\tau_0 d}{2dt}\int_0^1 q^2 dx - k\int_0^1 q_x\theta dx + \delta\int_0^1 q^2 dx = 0. \tag{3.54}$$

By equation $(3.40)_1$, we get

$$\psi_{tx} = \frac{\rho_1}{k}\varphi_{ttt}(x,t) + \frac{\mu_1}{k}\varphi_{tt}(x,t) - \varphi_{xxt}(x,t). \tag{3.55}$$

Now substituting ((3.55) in (3.52), we obtain

$$\begin{aligned}(3.50)_2 \Leftrightarrow \frac{\rho_1\rho_2}{2k}\frac{d}{dt}\int_0^1 \varphi_{tt}^2 dx + \frac{\rho_2}{2}\frac{d}{dt}\int_0^1 \varphi_{tx}^2 dx + \frac{b}{2}\frac{d}{dt}\int_0^1 \psi_x^2 dx \\ + k\int_0^1 (\varphi_x+\psi)\psi_t dx + \frac{\mu_1\rho_2}{k}\int_0^1 \varphi_{tt}^2 dx \\ + \gamma\int_0^1 \theta_x\psi_t dx + \frac{d}{dt}\int_0^1 \widehat{\mathrm{f}}(\psi)dx = 0.\end{aligned} \tag{3.56}$$

By summing the equations (3.51), (3.53), (3.54) and (3.56), we have

$$\begin{aligned}&\frac{d}{2dt}\left[\rho_1\int_0^1\varphi_t^2dx+k\int_0^1(\varphi_x+\psi)^2dx+\frac{\rho_1\rho_2}{K}\int_0^1\varphi_{tt}^2dx\right]\\&+\frac{d}{2dt}\left[\rho_2\int_0^1\varphi_{tx}^2dx+b\int_0^1\psi_x^2dx+\rho_3\int_0^1\theta^2dx+\tau_0\int_0^1q^2dx+2\widehat{\mathrm{f}}(\psi)\right]\\&+\mu_1\int_0^1\varphi_t^2dx+\frac{\mu_1\rho_2}{K}\int_0^1\varphi_{tt}^2dx+\delta\int_0^1q^2dx+\lambda\int_0^1\theta^2dx=0.\end{aligned}\tag{3.57}$$

By (3.58), obtaining (3.49). The proof of Lemma 3.4.1 is completed.

$$\begin{aligned}&\frac{d}{2dt}\left[\rho_1\int_0^1\varphi_t^2dx+k\int_0^1(\varphi_x+\psi)^2dx+\frac{\rho_1\rho_2}{k}\int_0^1\varphi_{tt}^2dx\right]\\&+\frac{d}{2dt}\left[\rho_2\int_0^1\varphi_{tx}^2dx+b\int_0^1\psi_x^2dx+\rho_3\int_0^1\theta^2dx+\tau_0\int_0^1q^2dx+2\widehat{\mathrm{f}}(\psi)\right]\\&=-\mu_1\int_0^1\varphi_t^2dx-\frac{\mu_1\rho_2}{k}\int_0^1\varphi_{tt}^2dx-\delta\int_0^1q^2dx-\lambda\int_0^1\theta^2dx.\end{aligned}\tag{3.58}$$

Which complete the proof. □

We need to introduce the following auxiliary Lemmas.

Lemma 3.4.2. *Let (φ,ψ,θ,q) be a solution for (3.40)-(3.27). The functional $\mathcal{F}_1(t)$ defined by*

$$\mathcal{F}_1(t)=-\frac{\mu_1}{2}\int_0^1\varphi_t^2dx-k\int_0^1\varphi_{tx}\varphi_xdx,\tag{3.59}$$

(3.60)

satisfies, for any $\varepsilon_1>0$, the following estimate

$$\mathcal{F}_1'(t)\le-k\int_0^1\varphi_{tx}^2dx+k\varepsilon_1\int_0^1\psi_x^2dx+\left(\rho_1+\frac{k}{4\varepsilon_1}\right)\int_0^1\varphi_{tt}^2dx.\tag{3.61}$$

Proof. Differentiating $\mathcal{F}_1$, we obtain

$$\mathcal{F}_1'(t)=-\mu_1\int_0^1\varphi_t\varphi_{tt}dx-k\int_0^1\varphi_{ttx}\varphi_xdx-k\int_0^1\varphi_{tx}^2dx.\tag{3.62}$$

Using $(3.40)_1$ and integrating by parts, we get

$$\mathcal{F}_1'(t)=\rho_1\int_0^1\varphi_{tt}^2dx-k\int_0^1\varphi_{tt}\psi_xdx-k\int_0^1\varphi_{tx}^2dx.\tag{3.63}$$

□

Proof. Direct computation using integration by parts, we get

$$\mathcal{F}_1'(t) = -\mu_1 \int_0^1 \varphi_t \varphi_{tt} dx - k \int_0^1 \varphi_{ttx} \varphi_x dx - k \int_0^1 \varphi_{tx}^2 dx. \tag{3.64}$$

Using (3.64) and the fact that

$$\varphi_t(x,t) = -\frac{\rho_1}{\mu_1} \varphi_{tt}(x,t) + \frac{k}{\mu_1} \left(\varphi_x + \psi\right)_x (x,t),$$

we obtain

$$\begin{aligned}
\mathcal{F}_1'(t) &= \rho_1 \int_0^1 \varphi_{tt}^2 dx - k \int_0^1 \left(\varphi_x + \psi\right)_x \varphi_{tt} dx - k \int_0^1 \varphi_{tx}^2 dx \\
&\quad - k \int_0^1 \varphi_{ttx} \varphi_x dx \\
&= \rho_1 \int_0^1 \varphi_{tt}^2 dx + k \int_0^1 \varphi_{ttx} \varphi_x dx - k \int_0^1 \varphi_{tx}^2 dx \\
&\quad - k \int_0^1 \varphi_{ttx} \varphi_x dx + k \int_0^1 \varphi_{ttx} \psi dx \\
&= \rho_1 \int_0^1 \varphi_{tt}^2 dx - k \int_0^1 \varphi_{tt} \psi_x dx - k \int_0^1 \varphi_{tx}^2 dx.
\end{aligned}$$

Using Young inequalities, we obtain (3.61). By applying Young's inequality (3.23), we obtain (3.61). □

Lemma 3.4.3. *Let $(\varphi, \psi, \theta, q)$ be a solution for (3.40)-(3.27). The functional $\mathcal{F}_2(t)$ defined by*

$$\begin{aligned}
\mathcal{F}_2(t) = -\rho_2 \int_0^1 \varphi_{tx} \psi dx + \frac{\mu_1}{2} \int_0^1 \varphi^2 dx + \rho_1 \int_0^1 \varphi_t \varphi dx \\
+ \frac{\rho_2 \rho_3}{\gamma} \int_0^1 \varphi_t \theta dx.
\end{aligned} \tag{3.65}$$

satisfies, $\forall t \geq 0$

$$\begin{aligned}
\mathcal{F}_2'(t) \leq -k \int_0^1 (\varphi_x + \psi)^2 dx - \frac{b}{2} \int_0^1 \psi_x^2 dx + \left(\rho_1 + \frac{\lambda \rho_2}{2\gamma}\right) \int_0^1 \varphi_t^2 dx \\
+ \frac{\rho_2 \rho_3}{2\gamma} \int_0^1 \varphi_{tt}^2 dx + \frac{k\rho_2}{2\gamma} \int_0^1 \varphi_{tx}^2 dx + \frac{k\rho_2}{2\gamma} \int_0^1 q^2 dx \\
+ \left(\frac{\gamma^2}{2b} + \frac{\rho_2}{2\gamma}(\rho_3 + \lambda)\right) \int_0^1 \theta^2 dx - \int_0^1 \widehat{\mathrm{f}}(\psi) dx.
\end{aligned} \tag{3.66}$$

Proof. By differentiating $\mathcal{F}_2$, we get

$$\begin{aligned}
\mathcal{F}_2'(t) = \rho_1 \int_0^1 \varphi_t^2 dx + \rho_1 \int_0^1 \varphi \varphi_{tt} dx + \mu_1 \int_0^1 \varphi \varphi_t dx - \rho_2 \int_0^1 \varphi_{ttx} \psi dx \\
- \rho_2 \int_0^1 \varphi_{tx} \psi_t dx + \frac{\rho_2 \rho_3}{\gamma} \int_0^1 \varphi_{tt} \theta dx + \frac{\rho_2 \rho_3}{\gamma} \int_0^1 \varphi_t \theta_t dx.
\end{aligned} \tag{3.67}$$

Using $(3.40)_1, (3.40)_2, (3.40)_3$ and integrating by parts, we obtain

$$\begin{aligned}\mathcal{F}_2'(t) = \rho_1 \int_0^1 \varphi_t^2 dx + \rho_2 \int_0^1 \varphi_t \psi_{tx} dx - b \int_0^1 \psi_x^2 dx \\ - k \int_0^1 (\varphi_x + \psi)^2 dx + \gamma \int_0^1 \theta \psi_x dx + \frac{\rho_2 \rho_3}{\gamma} \int_0^1 \varphi_{tt} \theta dx \\ + \frac{\rho_2 \rho_3}{\gamma} \int_0^1 \varphi_t \theta_t dx - \int_0^1 \psi \mathrm{f}(\psi) dx, \end{aligned} \tag{3.68}$$

by exploiting (3.21) in the last term of (3.68), we can write

$$\begin{aligned}\mathcal{F}_2'(t) \leq \rho_1 \int_0^1 \varphi_t^2 dx - k \int_0^1 (\varphi_x + \psi)^2 dx - b \int_0^1 \psi_x^2 dx - \frac{\rho_2 k}{\gamma} \int_0^1 \varphi_{tx} q dx \\ + \gamma \int_0^1 \theta \psi_x dx + \frac{\rho_2 \rho_3}{\gamma} \int_0^1 \varphi_{tt} \theta - \frac{\lambda \rho_2}{\gamma} \int_0^1 \varphi_t \theta dx - \int_0^1 \widehat{\mathrm{f}}(\psi) dx, \end{aligned}$$

and applying Young's inequality (3.23), we obtain (3.66). Differentiating $\mathcal{F}_2$ and integration by parts, we have

$$\begin{aligned}\mathcal{F}_2'(t) = \rho_1 \int_0^1 \varphi_t^2 dx + \rho_1 \int_0^1 \varphi \varphi_{tt} dx + \mu_1 \int_0^1 \varphi \varphi_t dx - \rho_2 \int_0^1 \varphi_{ttx} \psi dx \\ - \rho_2 \int_0^1 \varphi_{tx} \psi_t dx + \frac{\rho_2 \rho_3}{\gamma} \int_0^1 \varphi_{tt} \theta dx + \frac{\rho_2 \rho_3}{\gamma} \int_0^1 \varphi_t \theta_t dx. \end{aligned} \tag{3.69}$$

On the other hand, we have

$$\begin{cases} \varphi_t(x,t) & = -\frac{\rho_1}{\mu_1} \varphi_{tt}(x,t) + \frac{k}{\mu_1} (\varphi_x + \psi)_x (x,t), \\ \varphi_{ttx}(x,t) & = -\frac{b}{\rho_2} \psi_{xx}(x,t) + \frac{k}{\rho_2} (\varphi_x + \psi)(x,t) + \frac{\gamma}{\rho_2} \theta_x (x,t) \\ & \quad + \frac{1}{\rho_2} \mathrm{f}(\psi)(x,t), \\ \psi_{tx}(x,t) & = -\frac{\rho_3}{\gamma} \theta_t (x,t) - \frac{k}{\gamma} q_x (x,t) - \frac{\lambda}{\gamma} \theta (x,t). \end{cases} \tag{3.70}$$

(3.69)-(3.70) imply that

$$\begin{aligned}\mathcal{F}_2'(t) = \rho_1 \int_0^1 \varphi_t^2 dx + \rho_2 \int_0^1 \varphi_t \psi_{tx} dx - b \int_0^1 \psi_x^2 dx \\ - k \int_0^1 (\varphi_x + \psi)^2 dx + \gamma \int_0^1 \theta \psi_x dx - \int_0^1 \mathrm{f}(\psi) \psi dx \\ + \frac{\rho_2 \rho_3}{\gamma} \int_0^1 \varphi_{tt} \theta dx + \frac{\rho_2 \rho_3}{\gamma} \int_0^1 \varphi_t \theta_t dx, \end{aligned}$$

then

$$\begin{aligned}\mathcal{F}_2'(t) = \rho_1 \int_0^1 \varphi_t^2 dx - k \int_0^1 (\varphi_x + \psi)^2 dx - b \int_0^1 \psi_x^2 dx \\ + \rho_2 \int_0^1 \varphi_t \left(-\frac{\rho_3}{\gamma} \theta_t - \frac{k}{\gamma} q_x - \frac{\lambda}{\gamma} \theta \right) dx + \gamma \int_0^1 \theta \psi_x dx - \int_0^1 \psi \mathrm{f}(\psi) dx \\ + \frac{\rho_2 \rho_3}{\gamma} \int_0^1 \varphi_{tt} \theta dx + \frac{\rho_2 \rho_3}{\gamma} \int_0^1 \varphi_t \theta_t dx. \end{aligned} \tag{3.71}$$

Cauchy-Schwarz and Poincaré inequalities lead to

$$\begin{aligned}\int_0^1 |\mathrm{f}(\psi)\psi|dx &\leq \int_0^1 |\psi|^{\varrho}|\psi||\psi|dx \\ &\leq \|\psi\|^{\varrho}_{2(\varrho+1)}\|\psi\|_{2(\varrho+1)}\|\psi\|dx \\ &\leq c_1\int_0^1 \psi_x^2 dx, \end{aligned} \tag{3.72}$$

for some $k_1>0, k_2>0, c_1>0, c_2>0$

At this point, we distinguish two cases.

Case 1: If H is linear on$[0,\varepsilon]$. In this case, using the assumption (**??**), we can write

$$k_2\int_0^1 \mathrm{f}(\psi)^2\,dx \leq k_2\int_0^1 \left[\psi^2+\mathrm{f}(\psi)^2\right]dx \leq k_2\int_0^1 \psi\mathrm{f}(\psi) \leq -k_3\mathcal{E}'(t),$$

this inequality imply that

$$-\int_0^1 \mathrm{f}(\psi)^2\,dx \geq -\int_0^1 \psi\mathrm{f}(\psi). \tag{3.73}$$

By (3.71) and (3.73), we get

$$\begin{aligned}\mathcal{F}_2'(t) \leq \rho_1\int_0^1 \varphi_t^2 dx - k\int_0^1 (\varphi_x+\psi)^2 dx - b\int_0^1 \psi_x^2 dx - \frac{\rho_2 k}{\gamma}\int_0^1 \varphi_{tx}q dx \\ +\gamma\int_0^1 \theta\psi_x dx + \frac{\rho_2\rho_3}{\gamma}\int_0^1 \varphi_{tt}\theta - \frac{\lambda\rho_2}{\gamma}\int_0^1 \varphi_t\theta dx - \int_0^1 \psi\mathrm{f}(\psi)\,dx,\end{aligned}$$

then

$$\begin{aligned}\mathcal{F}_2'(t) \leq -k\int_0^1 (\varphi_x+\psi)^2 dx - \frac{b}{2}\int_0^1 \psi_x^2 dx + \left(\rho_1+\frac{\lambda\rho_2}{2\gamma}\right)\int_0^1 \varphi_t^2 dx \\ +\frac{\rho_2\rho_3}{2\gamma}\int_0^1 \varphi_{tt}^2 dx + \frac{k\rho_2}{2\gamma}\int_0^1 \varphi_{tx}^2 dx + \frac{k\rho_2}{2\gamma}\int_0^1 q^2 dx \\ +\left(\frac{\gamma^2}{2b}+\frac{\rho_2}{2\gamma}(\rho_3+\lambda)\right)\int_0^1 \theta^2 dx - \int_0^1 \psi\mathrm{f}(\psi)\,dx\end{aligned} \tag{3.74}$$

Choosing we obtaining (3.66). Finally we get the estimate (3.66).

□

Now, we define Lyapunov functional $\mathcal{L}(t)$ by

$$\mathcal{L}(t) = N\mathcal{E}(t) + N_1\mathcal{F}_1(t) + N_2\mathcal{F}_2(t), \tag{3.75}$$

where N, N_1 and N_2 are positive constants.

Lemma 3.4.4. *Let $(\varphi, \psi, \theta, q)$ be a solution for (3.40)-(3.27). Then, there exist two positive constants γ_1 and γ_2, such that the Lyapunov functional (3.75) satisfies*

$$\gamma_1 \mathcal{E}(t) \leq \mathcal{L}(t) \leq \gamma_2 \mathcal{E}(t), \forall t \geq 0, \tag{3.76}$$

and

$$\mathcal{L}'(t) \leq -\beta_1 \mathcal{E}(t), \forall t \geq 0. \tag{3.77}$$

Proof. From (3.75), we have

$$\begin{aligned} |\mathcal{L}(t) - N\mathcal{E}(t)| \leq & \frac{N_1\mu_1}{2}\int_0^1 \varphi_t^2 dx + N_1 k \int_0^1 |\varphi_{tx}\varphi_x| dx \\ & + \frac{N_2\mu_1}{2}\int_0^1 \varphi^2 dx + \frac{N_2\rho_2\rho_3}{\gamma}\int_0^1 |\varphi_t \theta| dx \\ & + N_2\rho_1 \int_0^1 |\varphi_t \varphi| dx + N_2\rho_2 \int_0^1 |\varphi_{tx}\psi| dx. \end{aligned} \tag{3.78}$$

By applying Young's (3.23), Poincaré (3.24) inequalities and exploiting (3.25) we arrive at

$$\begin{aligned} |\mathcal{L}(t) - N\mathcal{E}(t)| \leq & \delta_1 \int_0^1 \varphi_t^2 dx + \delta_2 \int_0^1 \varphi_{tx}^2 dx + \delta_3 \int_0^1 (\varphi_x + \psi)^2 dx \\ & + \delta_4 \int_0^1 \varphi_{tt}^2 dx + \delta_5 \int_0^1 \psi_x^2 dx + \delta_6 \int_0^1 \theta^2 dx \\ & + \delta_7 \int_0^1 q^2 dx + \delta_8 \int_0^1 \widehat{\mathrm{f}}(\psi) dx \\ & \leq C\mathcal{E}(t), \end{aligned} \tag{3.79}$$

in which δ_i (i $= 1, \ldots, 8$) are positive constants as in, [18, 31, 37, 46].

So it yields $(N - C)\mathcal{E}(t) \leq \mathcal{L}(t) \leq (N + C)\mathcal{E}(t)$, by choosing N (depending on N_1, N_2) sufficiently large we obtain (3.76).

Now, by differentiating $\mathcal{L}(t)$, exploiting (3.61), (3.66) and setting $\varepsilon_1 = \frac{1}{N_1}$, we get □

Proof. We define an appropriate Lyapunov functional as

$$\mathcal{L}(t) = N\mathcal{E}(t) + N_1\mathcal{F}_1(t) + N_2\mathcal{F}_2(t)$$

where N, N_1, N_2 are positive constants to be chosen properly later.

$$\begin{aligned}\mathcal{L}'(t) \leq & -\left[\mu_1 N - \left(\rho_1 + \frac{\lambda\rho_2}{2\gamma}\right) N_2\right] \int_0^1 \varphi_t^2 dx \\ & -\left[kN_1 - \frac{k\rho_2}{2\gamma} N_2\right] \int_0^1 \varphi_{tx}^2 dx \\ & -[kN_2] \int_0^1 (\varphi_x + \psi)^2 dx \\ & -[N_2] \int_0^1 \widehat{\mathrm{f}}(\psi) dx \\ & -\left[\frac{\mu_1\rho_2}{k} N - \left(\rho_1 + \frac{k}{4\varepsilon_1}\right) N_1 - \frac{\rho_2\rho_3}{2\gamma} N_2\right] \int_0^1 \varphi_{tt}^2 dx \\ & -\left[\frac{b}{2} N_2 - k\varepsilon_1 N_1\right] \int_0^1 \psi_x^2 dx \\ & -\left[\lambda N - \left(\frac{\gamma^2}{2b} + \frac{\rho_2}{2\gamma}(\rho_3 + \lambda)\right) N_2\right] \int_0^1 \theta^2 dx \\ & -\left[\delta N - \frac{k\rho_2}{2\gamma} N_2\right] \int_0^1 q^2 dx\end{aligned} \tag{3.80}$$

By setting $\varepsilon_1 = \frac{1}{N_1}$, thus, we arrive at following

$$\begin{aligned}\mathcal{L}'(t) \leq & -\left[\mu_1 N - \left(\rho_1 + \frac{\lambda\rho_2}{2\gamma}\right) N_2\right] \int_0^1 \varphi_t^2 dx \\ & -\left[kN_1 - \frac{k\rho_2}{2\gamma} N_2\right] \int_0^1 \varphi_{tx}^2 dx \\ & -kN_2 \int_0^1 (\varphi_x + \psi)^2 dx - N_2 \int_0^1 \widehat{\mathrm{f}}(\psi) dx \\ & -\left[\frac{\mu_1\rho_2}{k} N - \left(\rho_1 + \frac{kN_1}{4}\right) N_1 - \frac{\rho_2\rho_3}{2\gamma} N_2\right] \int_0^1 \varphi_{tt}^2 dx \\ & -\left[\frac{b}{2} N_2 - k\right] \int_0^1 \psi_x^2 dx - \left[\delta N - \frac{k\rho_2}{2\gamma} N_2\right] \int_0^1 q^2 dx \\ & -\left[\lambda N - \left(\frac{\gamma^2}{2b} + \frac{\rho_2}{2\gamma}(\rho_3 + \lambda)\right) N_2\right] \int_0^1 \theta^2 dx.\end{aligned} \tag{3.81}$$

□

We choose N_2 large enough such that

$$\frac{b}{2} N_2 - k > 0,$$

then we take N_1 large enough so that

$$kN_1 - \frac{k\rho_2}{2\gamma} N_2 > 0.$$

Once N_2 and N_1 are fixed, we pick N large enough (so that (3.76) remains valid) such that

$$\mu_1 N - \left(\rho_1 + \frac{\lambda\rho_2}{2\gamma}\right) N_2 > 0,$$

$$\frac{\mu_1\rho_2}{k} N - \left(\rho_1 + \frac{kN_1}{4}\right) N_1 - \frac{\rho_2\rho_3}{2\gamma} N_2 > 0,$$

$$\lambda N - \left(\frac{\gamma^2}{2b} + \frac{\rho_2}{2\gamma}(\rho_3 + \lambda)\right) N_2 > 0,$$

and

$$\delta N - \frac{k\rho_2}{2\gamma} N_2 > 0.$$

Finally, we obtain

$$\mathcal{L}'(t) \leq -\beta_1 \mathcal{E}(t), \forall t \geq 0, \tag{3.82}$$

where β_1 is a positive constant.

We are now ready to state and prove the following exponential stability result.

Theorem 3.4.5. *Let $(\varphi, \psi, \theta, q)$ be a solution for (3.40)-(3.27). Then, there exists two positive constants λ_0 and λ_1, sauch that the energy function (3.48) satisfies, for all $t \geq 0$,*

$$\mathcal{E}(t) \leq \lambda_0 e^{-\lambda_1 t}. \tag{3.83}$$

Proof. By using the estimation (3.77) and having in mind the equivalence of $\mathcal{E}(t)$ and $\mathcal{L}(t)$, we conclude that

$$\mathcal{L}'(t) \leq -\lambda_1 \mathcal{L}(t), \forall t \geq 0, \tag{3.84}$$

where $\lambda_1 = \frac{\beta_1}{k_2}$. A simple integration of (3.84) gives

$$\mathcal{L}(t) \leq -\mathcal{L}(0) e^{-\lambda_1 t}, t \geq 0.$$

Which yields the serial result (3.83). And by using the other side of the equivalence relation (3.76) again. The proof is complete. □

3.5 Numerical Approximation

In this section, we propose a numerical approximation to the solution of the continuous problem (3.40), with initial and boundary conditions (3.27). This method is constructed from the

backward Euler scheme in time and the standard finite element in space, we refer [24, 25]. Let us introduce the function $\widehat{\varphi} = \varphi_t$ and the weak form associated with the system (3.40), which is obtained by multiplying the equations by testing the functions tests χ, ζ, η, ξ in $H_0^1(0,1)$ and integrating by parts, we have

$$\begin{cases} \rho_1(\widehat{\varphi}_t, \chi) + k(\varphi_x, \chi_x) - k(\psi_x, \chi) + \mu_1(\widehat{\varphi}, \chi) = 0, \\ -\rho_2(\widehat{\varphi}_{tx}, \zeta) + b(\psi_x, \zeta_x) + k(\varphi_x, \zeta) + k(\psi, \zeta) + \gamma(\theta_x, \zeta) + (f(\psi), \chi) = 0, \\ \rho_3(\theta_t, \eta) + k(q_x, \eta) + \gamma(\psi_{tx}, \eta) + \lambda(\theta, \eta) = 0, \\ \tau_0(q_t, \xi) + \delta(q, \xi) + k(\theta_x, \xi) = 0. \end{cases} \tag{3.85}$$

Let $N \in \mathbb{N}^*$, we divide (partition) the interval $(0,1)$ into subintervals $I_l = (x_{l-1}, x_l)$ of length $h = 1/N$ with

$$0 = x_0 < x_1 < ... < x_N = 1.$$

We denote this partion by $S_h \subset H_0^1(0,1)$ the space of continuous piecewise linear functions defined on this partition.

Let $\Delta t = T/M$ be the time step size, where $T > 0$ is a given final time and M is a positive integer. Our finite element method using the backward Euler scheme is to find $\widehat{\varphi}_h^n, \psi_h^n, \theta_h^n, q_h^n \in S_h$, for $n = 1, 2, ..., M$ and all χ_h,ζ_h,η_h,$\xi_h \in S_h$. Thus we have

$$\begin{cases} \dfrac{\rho_1}{\Delta t}(\widehat{\varphi}^n - \widehat{\varphi}^{n-1}, \chi_h) + k(\varphi_x^n, \chi_{hx}) - k(\psi_x^n, \chi_h) + \mu_1(\widehat{\varphi}^n, \chi_h) = 0, \\ -\dfrac{\rho_2}{\Delta t}(\widehat{\varphi}_x^n - \widehat{\varphi}_x^{n-1}, \zeta_h) + b(\psi_x^n, \zeta_{xh}) + k(\varphi_x^n, \zeta_h) + k(\psi^n, \zeta_h) + \gamma(\theta_x^n, \zeta_h) \\ +(f(\psi^n), \chi_h) = 0, \\ \dfrac{\rho_3}{\Delta t}(\theta^n - \theta^{n-1}, \eta_h) + k(q_x^n, \eta_h) + \dfrac{\gamma}{\Delta t}(\psi_x^n - \psi_x^{n-1}, \eta_h) + \lambda(\theta^n, \eta_h) = 0, \\ \dfrac{\tau_0}{\Delta t}(q^n - q^{n-1}, \xi_h) + \delta(q^n, \xi_h) + k(\theta_x^n, \xi_h) = 0, \end{cases} \tag{3.86}$$

where $\varphi^n = \varphi^{n-1} + \Delta t \widehat{\varphi}^n$, $\varphi^0 = \varphi_0$, $\widehat{\varphi}^0 = \varphi_1$, $\psi^0 = \psi_0$, $\theta^0 = \theta_0$ and $q^0 = q_0$.

In order to find $\{\widehat{\varphi}^n, \psi^n, \theta^n, q^n\}$, we need to solve four coupled systems of algebraic equations with symmetric positive definite matrices (see remark 3.5.1). Therefore, we have a unique solution for a system. So, to solve the nonlinear problem (3.86), we use a fixed-point algorithm.

Then,

$$\begin{cases} ((1+\frac{\mu_1\Delta t}{\rho_1})\widehat{\varphi}^{n,j},\chi_h)=(\widehat{\varphi}^{n-1},\chi_h)-\frac{k\Delta t}{\rho_1}(\varphi_x^{n,j-1},\chi_{hx})+\frac{k\Delta t}{\rho_1}(\psi_x^{n,j-1},\chi_h), \\ k(\psi^{n,j},\zeta_h)+b(\psi_x^{n,j},\zeta_{xh})=\frac{\rho_2}{\Delta t}(\widehat{\varphi}_x^{n,j}-\widehat{\varphi}_x^{n-1},\zeta_h)-k(\varphi_x^{n,j},\zeta_h) \\ -\gamma(\theta_x^{n,j-1},\zeta_h)-(f(\psi^{n,j-1}),\chi_h), \\ \left((1+\frac{\lambda\Delta t}{\rho_3})\theta^{n,j},\eta_h\right)=(\theta^{n-1},\eta_h)-\frac{k\Delta t}{\rho_3}(q_x^{n,j-1},\eta_h)-\frac{\gamma}{\rho_3}(\psi_x^{n,j}-\psi_x^{n-1},\eta_h), \\ \left((1+\frac{\delta\Delta t}{\tau_0})q^{n,j},\xi_h\right)=(q^{n-1},\xi_h)-\frac{\kappa\Delta t}{\tau_0}(\theta_x^{n,j},\xi_h), \end{cases} \tag{3.87}$$

where $\varphi^{n,0}=\varphi^{n-1}$, $\widehat{\varphi}^{n,0}=\widehat{\varphi}^{n-1}$, $\psi^{n,0}=\psi^{n-1}$, $\theta^{n,0}=\theta^{n-1}$, $q^{n,0}=q^{n-1}$ and $\varphi^{n,j}=\varphi^{n-1}+\Delta t\widehat{\varphi}^{n,j}$.

In any case, we solve the well-posed problem (3.87) by repeated (iterative) procedure which is stopped when the difference between two successive iterations became less than a tolerance ε.

Remark 3.5.1. Let $\chi_h=\zeta_h=\eta_h=\xi_h\in S_h=vect\{V_1,V_2,..,V_N\}$. The method defined in this thesis requires that the systems of algebraic equations

$$\begin{cases} (1+\frac{\mu_1\Delta t}{\rho_1})\mathbf{A}\widehat{\Phi}^{n,j}=\mathbf{A}\widehat{\Phi}^{n-1}-\frac{k\Delta t}{\rho_1}\mathbf{B}\Phi^{n,j-1}+\frac{k\Delta t}{\rho_1}\mathbf{C}\Psi^{n,j-1}, \\ (k\mathbf{A}+b\mathbf{B})\Psi^{n,j}=\frac{\rho_2}{\Delta t}\mathbf{C}\left(\widehat{\Phi}^{n,j}-\widehat{\Phi}^{n-1}\right)-k\mathbf{C}\Phi^{n,j}-\gamma\mathbf{C}\Theta^{n,j-1} \\ -\mathbf{A}(\mathbf{f}(\Psi^{n,j-1})), \\ (1+\frac{\lambda\Delta t}{\rho_3})\mathbf{A}\Theta^{n,j}=\mathbf{A}\Theta^{n-1}-\frac{k\Delta t}{\rho_3}\mathbf{C}Q^{n,j-1}-\frac{\gamma}{\rho_3}\mathbf{C}(\Psi^{n,j}-\Psi^{n-1}), \\ (1+\frac{\delta\Delta t}{\tau_0})\mathbf{A}Q^{n,j}=\mathbf{A}Q^{n-1}-\frac{k\Delta t}{\tau_0}\mathbf{C}\Theta^{n,j}, \end{cases}$$

where $\mathbf{A}_{ie}=(V_i,V_e)$, $\mathbf{B}_{ie}=\left(\frac{d}{dx}V_i,\frac{d}{dx}V_e\right)$, $\mathbf{C}_{ie}=\left(\frac{d}{dx}V_i,V_e\right)$ $(i,e=1,2,...,N)$,

and

$$\varphi^{n,j}=\sum_{i=1}^{N}\Phi_i^{n,j}V_i,\ \widehat{\varphi}^{n,j}=\sum_{i=1}^{N}\widehat{\Phi}_i^{n,j}V_i,\ \psi^{n,j}=\sum_{i=1}^{N}\Psi_i^{n,j}V_i,\ \theta^{n,j}=\sum_{i=1}^{N}\Theta_i^{n,j}V_i$$
$$q^{n,j}=\sum_{i=1}^{N}Q_i^{n,j}V_i.$$

To compute the integral $I=\int_0^1 g(x)dx$, we use the trapezoidal quadrature formula:

$$I_N=\sum_{i=1}^{N}w_ig(x_i)\approx I,$$

where the weights $\{w_i\}_{i=1}^{N}$ are given by $w_1=w_N=h/2$ for $i=1,N$ and $w_i=h$, for $i=2,3,...,N-1$,

The formula for calculating for (computation) the approximate energy using trapezoidal quadrature is given by

$$\begin{aligned}\varepsilon(t^n) \approx E^n = 1/2\sum_{i=1}^{N} w_i[&\rho_1\varphi_t^2(x_i,t^n) + k(\varphi_x(x_i,t^n)+\psi(x_i,t^n))^2\\ &+\frac{\rho_1\rho_2}{k}\varphi_{tt}^2(x_i,t^n) + b\psi_x^2(x_i,t^n) + \rho_3\theta^2(x_i,t^n) + \tau_0 q^2(x_i,t^n)\\ &+2f(\psi(x_i,t^n))],\end{aligned} \tag{3.88}$$

where

$\varphi_t(x_i,t^n) = \widehat{\varphi}(x_i,t^n)$, $\varphi_{tt}(x_i,t^n) = \dfrac{1}{\Delta t}(\widehat{\varphi}(x_i,t^{n+1}) - \widehat{\varphi}(x_i,t^n))$,

$\varphi_x(x_i,t^n) = \dfrac{1}{h}(\varphi(x_{i+1},t^n) - \varphi(x_i,t^n))$ and $\psi_x(x_i,t^n) = \dfrac{1}{h}(\psi(x_{i+1},t^n) - \psi(x_i,t^n))$.

Example (1). Let $f(z) = z^2 + 2z^3$ and $\rho_1 = 1.75$, $\rho_2 = 1.5$, $\rho_3 = 1$, $\delta = 0.015$, $k = 0.000035$, $\mu_1 = 0.35$, $b = 4$, $\gamma = 0.001$, $\tau_0 = 0.4$, $\lambda = 0.8$ and $\varepsilon = 10^{-6}$. The discretization parameters are fixed equal to $N = 100$, $M = 1000$ with he final time $T = 100$ and the initial data

$$\varphi_0 = 250x(1-x),\ \varphi_1 = \theta_0 = x(1-x)^2\sin(x),\ \psi_0 = x(1-x)\exp(x^2)$$
$$\text{and } q_0 = x(1-x).$$

Example (2). Let $f(z) = \cos(z^2)$ and $\rho_1 = 2$, $\rho_2 = 1.2$, $\rho_3 = 1.5$, $\delta = 0.035$, $k = 0.0001$, $\mu_1 = 0.75$, $b = 2$, $\gamma = 0.001$, $\tau_0 = 0.25$, $\lambda = 0.75$ and $\varepsilon = 10^{-6}$. The discretization parameters are fixed equal to $N = 100$, $M = 1000$ with the final time $T = 100$ and the initial data

$$\varphi_0 = x^3(1-x)^2,\ \varphi_1 = 10x(1-x),\ \psi_0 = x\cos(2\pi x),\ \theta_0 = \frac{1}{10}x(1-x)$$
$$\text{and } q_0 = (1-x)\sin(2\pi x).$$

In each above numerical example, the graphics presented in the Figures (1-4), (6-9) show the decreasing of the functions φ, ψ, θ and q on the interval $]t_0, T]$ with $t_0 > 0$, for different choices of the system parameters and of the initial data. Furthermore, the Figures 5 and 10 show that the approximate energy (3.88) decays in exponential manner which confiérms the main theoretical result obtained in section 3.

3.5.1 Conclusion

In this work, we studied the nonlinear Bresse-Timoshenko system with second sound and we showed that the dissipation given by this complementary control combining with the temper-

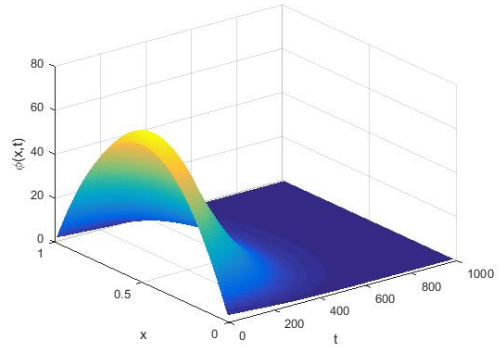

Figure 3.1: (Example 1) Approximation of function φ .

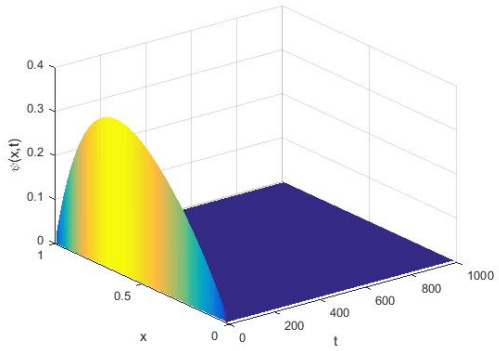

Figure 3.2: (Example 1) Approximation of function ψ .

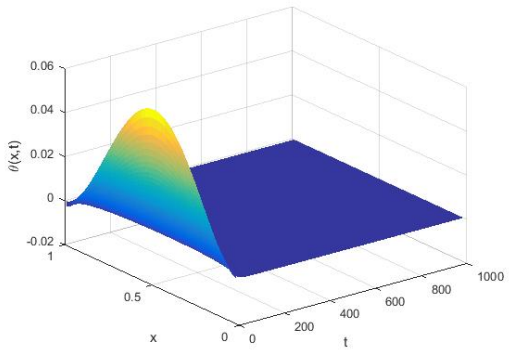

Figure 3.3: (Example 1) Approximation of function θ .

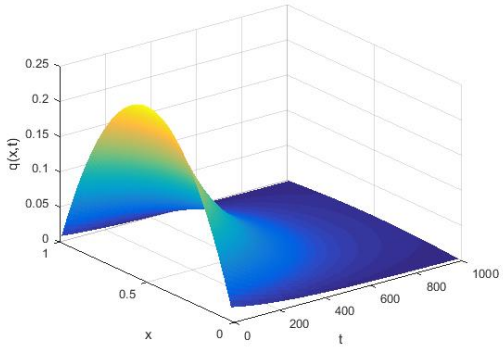

Figure 3.4: (Example 1) Approximation of function q .

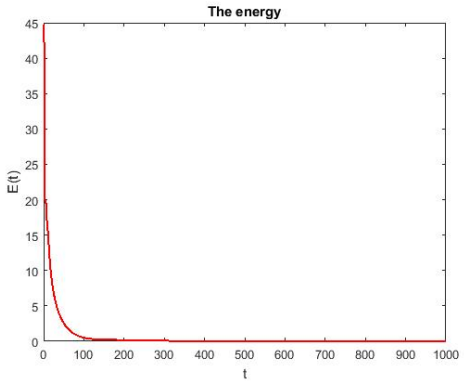

Figure 3.5: (Example 1) Approximation of the energy.

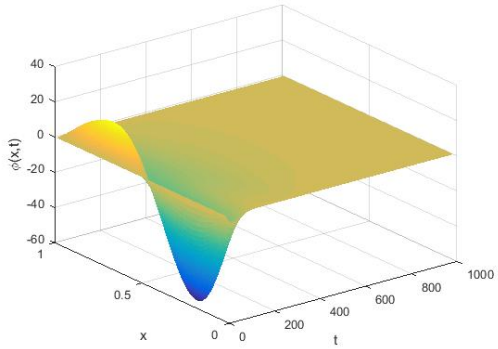

Figure 3.6: (Example 2) Approximation of function φ .

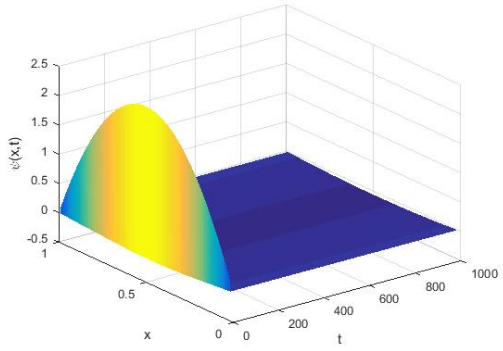

Figure 3.7: (Example 2) Approximation of function ψ .

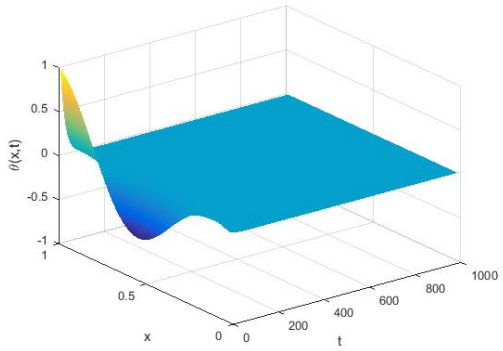

Figure 3.8: (Example 2) Approximation of function θ .

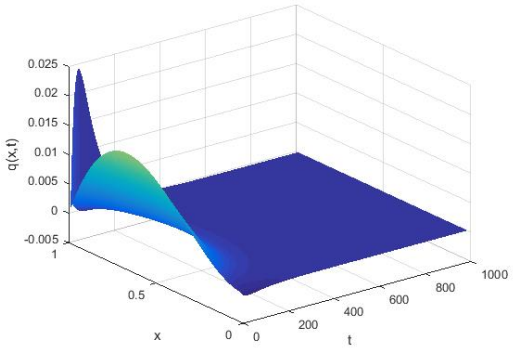

Figure 3.9: (Example 2) Approximation of function q .

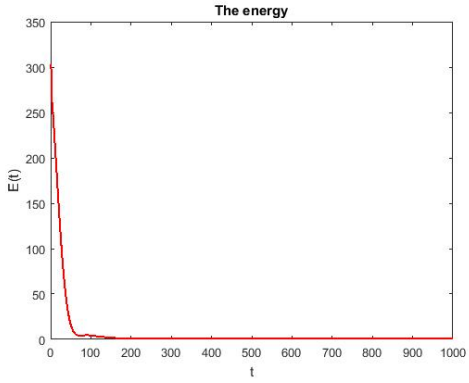

Figure 3.10: (Example 2) Approximation of the energy.

ature effect allow to stabilize exponentially the system. Moreover, the numerical tests that have been performed conérm the asymptotic behavior of the energy. In the future, we will consider another mechanism damping such that the microtemperature to study the stability of Bresse-Timoshenko system. The problem in question is the following system

$$\begin{cases} \rho_1\varphi_{tt} - k\left(\varphi_x + \psi\right)_x = 0 & \text{in} \quad (0,1)\times(0,\infty), \\ -\rho_2\varphi_{ttx} - b\psi_{xx} + k\left(\varphi_x + \psi\right) + \gamma\omega_x = 0 & \text{in} \quad (0,1)\times(0,\infty), \\ \rho_3\omega_t - k_1\omega_{xx} + \lambda\omega - \gamma\psi_{tx} = 0 & \text{in} \quad (0,1)\times(0,\infty), \end{cases} \tag{3.89}$$

in this case the situation is different and more complicated than the problem (3.40) because in this case one we considered a single term of dissipation given by the microtemperature.

Bibliography

[1] R. A. Adams, sobolev spaces, Academic Press, New York, 1975, 286 p.

[2] S. Adjemi, A. Berkane, S. Zitouni, T. Bechouat, Exponential decay and numerical solution of nonlinear Bresse-Timoshenko system with second sound. Journal of Thermal Stresses, (2022), 154- 170, DOI: 10.1080/01495739.2022.2030838.

[3] E. Alexandre, J. L. Guermand, ElÃľment finis : thÃľorie, application, mise en oeuvre. Springer-Verlag, Berlin, volume (36), 2002.

[4] D. Andrade, M. A. Jorge Silva, T. F. Ma, Exponential stability for a plate equation with p-Laplacian and memory terms, Math. Methods Appl. Sci, 4 (2012), 417-426.

[5] M. Aouadi, A. Castejon, Properties of global and exponential attractors for nonlinear thermo-diffusion Timoshenko system, J. Math. Phys., 60 (2019), 1-26.

[6] D. S. Almeida Junior, A. J. A. Ramos, On the nature of dissipative Timoshenko systems at light of the second spectrum. Z. Angew. Math. Phys. 68 (2017), 1-31.

[7] D. S. Almeida Junior, I. Elishakoff, A. J. A. Ramos, L. G. Rosï£¡rio Miranda, The hypothesis of equal wave speeds for stabilization of Timoshenko beam is not necessary anymore: the time delay cases. IMA Journal of Applied Mathematics, 00 (2019), 1-34.

[8] D. S. Almeida Junior, I. Elishakoff, A. J. A. Ramos, R. M. L. Gutemberg, The hypothesis of equal wave speeds for stabilization of Bresse-Timoshenko system is not necessary anymore, The time delay cases. IMAJ. Appl. Math, 84 (2019), 763-796.

[9] D. S. Almeida Junior, A. J. A. Ramos, M. L. Santos, R. M. L. Gutemberg, Asymptotic behavior of weakly dissipative Bresse-Timoshenko system on influence of the second spectrum of frequency. Z. Angew. Math. Mech, 98 (2018), 1320-1333.

[10] M. O. Alves, A. H. Caixeta, M. A. Jorge Silva, J. H. Rodrigues, D. S. Almeida Jénior, OnaTimoshenko system with thermal coupling on both the bending moment and the shear force. Journal of Evolution Equations, (2019), 1-27 doi.org/10.1007/s00028-019-00522-8.

[11] T. A. Apalaraa, S. A. Messaoudi, A. A. Keddi, On the decay rates of Timoshenko system with second sound. Math. Appl. Sci. 39 (2016), 2671-2684.

[12] J. Awrejcewicz, A. V. Krysko, V. Soldatov, V. A. Krysko, Analysis of the nonlinear dynamics of the Timoshenko flexible beams using wavelets. J. Comput. Nonlinear Dyn. 7 (2012), 1-14.

[13] J. Awrejcewicz, A. V. Krysko, S. P. Pavlov, M. V. Zhigalov, V. A. Krysko, Stability of the Size-Dependent and Functionally Graded Curvilinear Timoshenko Beams. J. Comput. Nonlinear Dyn. 12 (2017), 041018-8.

[14] J. Awrejcewicz, A. V. Krysko, S. P. Pavlov, M. V. Zhigalov, V. A. Krysko, Chaotic dynamics of size dependent Timoshenko beams with functionally graded properties along their thickness. Mechanical Systems and Signal Processing, 93, C, (2017), 415-430.

[15] J. Awrejcewicz, V. A. Krysko, S. P. Pavlov, M. V. Zhigalov, L. A. Kalutsky, A. V. Krysko, Thermoelastic vibrations of Timoshenko microbeam based on the modified couple stress theory. Nonlinear Dyn., 99 (2020), 919-943.

[16] J. Awrejcewicz, V. A. Krysko, I. V. Papkova, A. V. Krysko, Deterministic Chaos in One-Dimensional Continuous Systems. World Scientific Series on Nonlinear Science Series 90 (2016).

[17] M. Badr Benboubker, On Some Quasilinear Elliptic Nonhomogeneous Problems of Dirichlet or Neumann Type, Ph.D. Thesis, Sidi Mohamed Ben Abdellah University, 2014.

[18] S. Boulechfar, S. Zitouni, A. Djebabla, A. Guesmia, Energy decay of the Bresse system by tow thermos-viscolastic dampings. Nonlinear studies, 27 (2020), 957-974.

[19] J. A. C. Bresse, Cours de Mécanique Appliquée, Mallet-Bachelier, Paris, (1859).

[20] H. Brezis, Functional Analysis, Sobolev Spaces and Partial Differential Equations, Springer New York Dordrecht Heidelberg London (2010).

[21] H. Brézis, Analyse Fonctionnelle, Théorie et applications, Paris, 1983.

[22] A. Choucha, D. Ouchenane, Kh. Zennir, B. Feng, Global well-posedness and exponential stability results of a class of Bresse-Timoshenko-type systems with distributed delay term, Math. Methods Appl. Sci, (2020), 1-26.

[23] R. E. Edwards, Functional Analysis, Theory and Applications, Holt, Rinehart and Winston, New York, 1965.

[24] T. EL Arwadi, M. I. M. Copetti, W. Youssef, On the theoretical and numerical stability of the thermoviscoelastic Bresse system. Z. Angew. Math. Mech, 99 (2019), 1-20.

[25] M. Elhindi, Kh. Zennir, D. Ouchenane, A. Choucha, T. El Arwadi, Bresse-Timoshenko type systems with thermodiffusion effects: well-possedness, stability and numerical results. Rendiconti del Circolo Matematico di Palermo Series 2, (2021), 1-27. doi.org/10.1007/s12215-021-00672-0.

[26] I. Elishakoff, An equation both more consistent and simpler than the Bresse-Timoshenko equation, In Advances in mathematical modeling and experimental methods for materials and structures. SMIA, Springer, Berlin, 168 (2010), 249-254.

[27] I. Elishakoff, J. Kaplunov, E. Nolde, Celebrating the centenary of Timoshenko's study of effects of shear deformation and rotary inertia. ASME Am. Soc. Mech. Eng. Appl. Mech. Rev. 67 (2015), 1-11.

[28] I. Elishakoff, F. Hache, N. Challamel, Critical contrasting of three versions of vibrating Bresse-Timoshenko beam with a crack. Int. J. Solids Struct. 109 (2017) 143-151.

[29] B. Feng, D. S. Almeida Junior, M. J. dos Santos, L. G. Rosério Miranda, A new scenario for stability of nonlinear Bresse-Timoshenko type systems with time dependent delay, (2019), 1-17, DOI: 10.1002/zamm. 201900160.

[30] B. W. Feng, M. Pelicer, Global existence and exponential stability for a nonlinear Timoshenko system with delay. Boundary Value Problems, 206 (2015), 1-13.

[31] F. Foughali, S. Zitouni, H. E. Khochemane, A. Djebabla, Well-posedness and exponential decay for a porous-thermoelastic system with second sound and distributed delay. MESA. 11 (2020) 1003-1020.

[32] J. Genet, Mesure et intégrations théorie élémentaire, Librairie vuibert, 63, bd Saint-Germain, 75005 Paris, 1976.

[33] M. Houasni, S. Zitouni, R. Amiar, General decay for a viscoelastic damped Timoshenko system of second sound with distributed delay. MESA. 10 (2019), 323-340.

[34] M. Houasni, S. Zitouni, R. Amiar, Exponential decay for a thermo-viscoelastic Bresse system with second sound and delay terms, International Journal of Maps in Mathematics (IJMM), 3 (2020), 39-56.

[35] A. A. Keddi, T. A. Apalara, S. A. Messaoudi, Exponential and Polynomial Decay in a Thermoelastic-Bresse System with Second Sound. Appl. Math. Optim. 77 (2018), 315-341.

[36] Z. Khelifa, calcul intégral des Fonctions de plusieurs variables (LIVRE 13) ,université d'oron - Alger, O.P.U, 2014.

[37] H. E. Khochemane, L. Bouzettouta, S. Zitouni, General decay of a nonlinear damping porous-elastic system with past history. Annali Dell-universita- di Ferrara, Universit'a degli Studi di Ferrara, (2019). DOI : 10.1007/s11565-019-00321-6.

[38] H. E. Khochemane, A. Djebabla, S. Zitouni, L. Bouzettouta, Well-posedness and general decay of a nonlinear damping porous-elastic system with infinite memory. Journal of mathematical physics 61 (2020). doi:10.1063/1.5131031.

[39] V. A. Krysko, J. Awrejcewicz, M. V. Zhigalov, I. V. Papkova, T. V. Yakovleva, A. V. Krysko, On the mathematical models of the Timoshenko-type multi-layer flexible orthotropic shells. Nonlinear Dyn., 92 (2018), 2093-2118.

[40] O. A. Ladyzhenskaya, N. Ural-tseva, Linear and Quasilinear Elliptic Equations, Academic Press, New York, 1968.

[41] J. L. Lions, Quelques méthodes de résolution des problémes aux limites non linéaires, Dunod, Paris, 1969.

[42] R, Lord. The Theory of Sound. London: Macmillan, 1877?1878 (see also Dover, New York, 1945).

[43] T. Marie, S. Lacroix, Distributions-Espaces de Sobolev-Applications, Paris, 1986.

[44] F. Mokhtari, Nonlinear anisotropic parabolic equations in $\mathbb{R}^N$ with locally integrable data. Mathematical Methods in the Applied Sciences, 36 (2), 196-207, 2013.

[45] F. Mokhtari, Problémes paraboliques anisotropes et données dans un espace d Orlicz ou mesures, Thése de Doctorat, ENS, Département de Mathématiques, Vieux Kouba, Alger, Algérie, 2011.

[46] D. Ouchenane, R. Abdelaziz, general decay result of the Timoshenko system in thermoelasticity of second sound. Electronic Journal of Mathematical Analysis and Applications, 6 (2018), 45-64.

[47] M. A. J. Silva, T. F. Ma, On a viscoelastic plate equation with history setting and perturbation of p-Laplacian type. IMA J. Appl. Math, 78 (2013), 1130-1146.

[48] S. Timoshenko, On the correction for shear of the differential equation for transverse vibrations of prismatic bars. Philosophical Magazine, 41 (1921), 744-746.

[49] SP, Timoshenko. The Collected Papers. New York: McGraw-Hill, 1953.

[50] R. WYM, A manual of applied mechanics. London: R. Griffin and Co Ltd, 1858, 342-344.

[51] Kh. Zennir, D. Ouchenane, A. Choucha and M. Biomy, Well-posedness and stability for Bresse-Timoshenko type systems with thermodiffusion effects and nonlinear damping. AIMS Mathematics, 6 (2021), 2704-2721.

[52] S. Zitouni, L. Bouzettouta, Kh. Zennir and D. Ouchenane, Exponential decay of thermoelastic-Bresse system with distributed delay, Hacettepe Journal of Mathematics and Statistics Volume 47 (2018), 1216 -1230.

[53] O. C. Zienkiewicz, R. L. Taylor The finite Element Method, basic formulation and linear problems. McGraw-Hill, tome 1, 1989